Fitness advantage of *Bacteroides thetaiotaomicron* capsular polysaccharide is dependent on the resident microbiota

Authors:

- Hoces, Daniel[1]
- Greter, Giorgia[1]
- Arnoldini, Markus[1]
- Moresi, Claudia[1]
- Berent, Sara[1]
- Kolinko, Isabel[1]
- Bansept, Florence[3,#a]
- Woller, Aurore[3,#b]
- Häfliger, Janine[1, #c]
- Martens, Eric[4]
- Hardt, Wolf-Dietrich[2]
- Loverdo, Claude[3]
- Slack, Emma[1]

1. Institute of Food, Nutrition and Health, Department of Health Sciences and Technology, ETH Zürich, Zürich, Switzerland
2. Institute of Microbiology, Department of Biology, ETH Zürich, Zürich, Switzerland
3. Laboratoire Jean Perrin, Sorbonne Université/CNRS, Paris, France
4. Department of Microbiology and Immunology, University of Michigan Medical School, Ann Arbor, MI 48109, USA

[#a]Current address: Department for Evolutionary Theory, Max Planck Institute for Evolutionary Biology, Plön, Germany

[#b]Current address: Department of Molecular Cell Biology, Weizmann Institute of Science, Rehovot, Israel

[#c]Current address: Klinik für Gastroenterologie und Hepatologie, University Hospital Zurich, Zurich, Switzerland

1 Summary

2 Many microbiota-based therapeutics rely on our ability to introduce a microbe of choice into an
3 already-colonized intestine. However, we remain largely blind to the quantitative effects of
4 processes determining colonization success. In this study, we used genetically-barcoded
5 *Bacteroides thetaiotaomicron* (*B.theta*) strains in combination with mathematical modeling to
6 quantify population bottlenecks experienced by *B.theta* during gut colonization. Integrating
7 population bottlenecks sizes with careful quantification of net growth rates *in vivo* and *in vitro*
8 allows us to build models describing the events during intestinal colonization in the context of
9 gnotobiotic and complex microbiotas. Using these models, we estimated the decrease in niche
10 size for *B.theta* colonization with increasing microbiota complexity. In addition, our system can
11 be applied to mechanistically dissect colonization defects of mutant strains. As a proof of
12 concept, we demonstrated that the competitive disadvantage of a *B.theta* mutant lacking
13 capsular polysaccharide is due to a combination of an increased lag-phase before growth
14 initiation in the gut, combined with an increased clearance rate. Crucially, the requirement for
15 the *B.theta* capsule depended strongly on microbiota composition, suggesting that the
16 dominant role may be protection from bacterial or phage aggression rather than from host-
17 induced bactericidal mechanisms.

Introduction

19 From the moment that we first contact microbes at birth, we continuously encounter
20 environmental and food-borne microbes. Whether such encounters are transient or will lead to
21 long-term colonization, is influenced by complex ecological interactions between the invading
22 species and the existing consortium, as well as the host's dietary habits and the physiology of
23 the intestine (David et al., 2014; Wotzka et al., 2019). A better understanding of the factors
24 determining colonization efficiency is crucial in the development of microbiota engineering
25 strategies (Donia, 2015; Pham et al., 2017; Sheth et al., 2016) and in the use of bacterial
26 species as biosensors to probe microbiota function and stability (Goodman et al., 2009).

27 One established way of studying ecological processes within hosts is genetic barcode tagging
28 of otherwise isogenic microbes, which has previously been used to study population dynamics
29 of pathogens such as *Vibrio cholerae* or *Salmonella* Typhimurium within the infected host (Abel
30 et al., 2015b; Vlazaki et al., 2019). Based on barcode tagging and mathematical modelling, it
31 has been possible to infer parameters such as growth, clearance and migration rates
32 (Dybowski et al., 2015; Grant et al., 2008; Kaiser et al., 2014, 2013), as well as the size of
33 population bottlenecks imposed during colonization (Abel et al., 2015a; Li et al., 2013; Moor et
34 al., 2017), antibiotic treatment (Vlazaki et al., 2020) or immunity (Coward et al., 2014;
35 Hausmann et al., 2020; Lim et al., 2014; Maier et al., 2014; Moor et al., 2017). Furthermore,
36 combining neutral genetic barcodes with targeted mutant strains, this experimental tool can be
37 used to mechanistically analyze the fitness-effect of individual genes that regulate successful
38 gut colonization or tissue invasion (Di Martino et al., 2019; Nguyen et al., 2020).

39 In order to study the dynamics of invasion of a novel microbiota member, we chose to use
40 *Bacteroides thetaiotaomicron* (*B.theta*) as a model microbe. *B. theta* is a common commensal
41 member of the human intestinal microbiota (Porter et al., 2018), and a well-established toolbox
42 exists for engineering its genome (Porter et al., 2017; Whitaker et al., 2017). A common feature
43 of *Bacteroides* species is the ability use phase variation to modulate the expression of 3-10
44 capsular polysaccharide (CPS) operons, leading to the production of distinct capsule
45 structures (Porter and Martens, 2017). *B.theta* strains lacking a capsule have been shown to
46 engraft poorly in an existing microbiota when competing with CPS-expressing strains (Martens
47 et al., 2009; Porter et al., 2017). Critically for our studies, the deletion of all capsule gene
48 clusters is not expected to negatively influence the growth rate of *B.theta* per se (Rogers et al.,
49 2013) but is expected to affect survival on exposure to noxious stimuli, like bile acids, stomach
50 acid, antimicrobial peptides, or phage (Porter et al., 2020, 2017), making this a good model to
51 test our ability to quantify population dynamics *in vivo*. *B. theta* is also a relevant bacterium to
52 understand population dynamics of colonization, as its ability to colonize to very high densities

53   and the availability of precise tools for genetically engineering it (Lim et al., 2017; Mimee et al.,
54   2015) make it a strong candidate for introducing novel functions into microbiomes.

55   To quantify the processes determining success of *B.theta* colonization in the presence of
56   different resident microbiota, we generated genetically tagged *B.theta* strains with and without
57   capsule. Using a combination of mathematical modeling and experimental quantification of
58   population dynamics parameters, we estimated the probability of colonization success during
59   single-strain colonization and competition. This revealed that acapsular *B.theta* have similar
60   colonization success (i.e., encounter similar population bottlenecks) to wild-type strains when
61   invading gnotobiotic microbiota communities, but not when invading a more complete
62   microbiome. However, the acapsular strain still competes poorly with the wild-type strain in co-
63   colonization even in gnotobiotic settings. The underlying mechanisms depend upon the
64   increased clearance and extended lag-phase of the acapsular *B.theta in vivo*. Therefore,
65   neutral tagging and mathematical modeling can be used to infer behavior of *B.theta* and
66   protective functions of the polysaccharide capsule in a mouse model.

Results

Genetically-tagged *B.theta* strains to study within-host population dynamics

We first established tools that would allow us to quantify *B.theta* clonal loss *in vivo* and to test the plausibility of our theoretical models. Briefly, we used the previously described pNBU2 integration plasmid carrying an antibiotic resistance cassette, a phage promoter and an optimized ribosome binding site for fluorescent protein expression which allows visualization of clones (Wang et al., 2000; Whitaker et al., 2017). Six barcode tags, previously developed and validated for *Salmonella* (Wild-type Isogenic Tagged Strains, WITS (Grant et al., 2008; Maier et al., 2013) were inserted into an erythromycin-resistant (*ermG* cassette (Cheng et al., 2000) pNBU2 vector (Fig.1A). These six tags were inserted in both *B.theta* VPI-5482 *Δtdk*, which can phase vary the expression of eight different capsular polysaccharides (*B.theta* WT); and a *B.theta* strain that cannot produce capsule, generated by sequentially deleting all CPS gene clusters (*B.theta* acapsular) (Porter et al., 2017). A matched set of strains was produced in which an identical pNBU2-derived plasmid was integrated carrying the *tetQb* resistant cassette (Nikolich et al., 1992) in place of *ermG,* conferring instead tetracycline resistance (TetR). All strains also express a fluorescent protein, either GFP or mCherry (Fig.1A, Suppl.Table 1).

**Genetic barcode tags do not affect fitness of *B.theta* strains**

A critical assumption of any analysis using genetically barcoded strains is that the chromosomal insertions, as well as the construction process, have not altered the fitness of the strains compared to the wild-type, both in culture and when colonizing a host. When grown individually in BHIS media, the *B.theta* strains carrying the different barcode tags had a similar growth rate (median doubling time ranged from 78-90 min) (Fig.1B and Suppl. Fig.1A). Also, they maintained their relative abundances, evaluated by qPCR (Fig.1C), when mixed and grown overnight (Suppl.Fig.1B and Suppl.Fig.1C).

To test whether the tags confer a fitness effect upon colonization of a host, we colonized germ-free mice with a uniform mixture of 10^7 colony forming units (CFU) of each tagged strain (Fig.1D). At this tag abundance, stochastic loss of tags is highly unlikely. We compared the relative abundance of each tag in the inoculum to that in the cecal content and feces after 48h of colonization. These experiments revealed small, random deviations in the distribution, consistent with uniform fitness (Fig.1E). Finally, as erythromycin- and tetracycline-resistance were used to distinguish the tagged and untagged *B.theta* strains, we also tested whether the antibiotic resistant cassettes alter competitive fitness and found no significant difference between strains carrying the two resistance cassettes in culture (Fig.1F) or upon colonization (Suppl. Fig.1D).

5
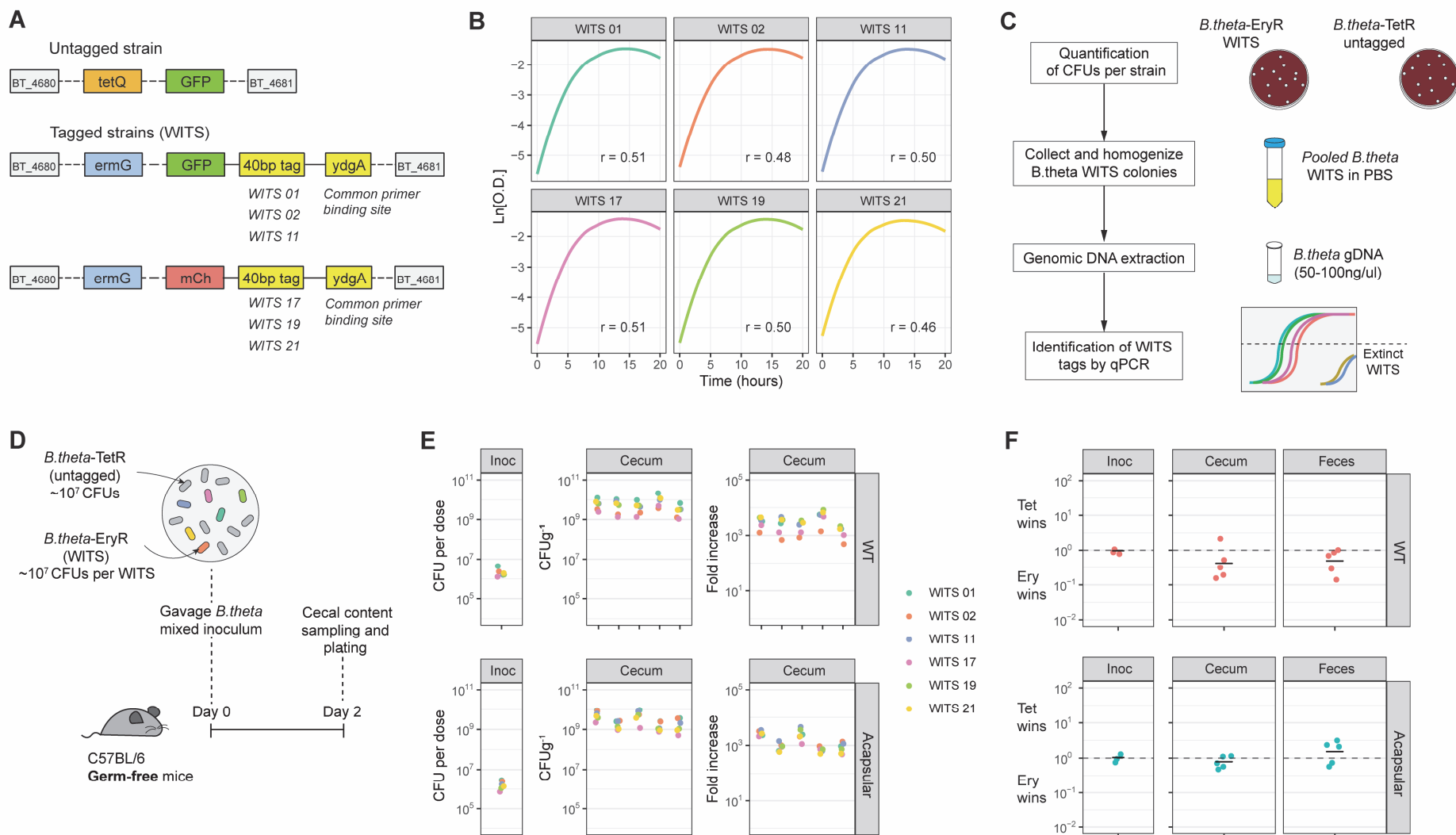
Figure 1: Tagged *B.theta* strains have similar fitness for growing *in vitro* and *in vivo*. (A) Schematic representation of insertions in *B.theta* genome. **(B)** Growth curves of *B.theta* WT in BHIS media (n=3 per strain) and growth rates (r, hours⁻¹) per tag. **(C)** Workflow for sample preparation and data acquisition. **(D)** Experimental design of *in vivo* competitions. All strains (untagged *B.theta*-TetR and all six tagged *B.theta*-EryR WITS) were mixed in a 1:1 ratio. **(E)** Tags distribution during colonization among six *B.theta* tagged strains either WT or acapsular. Plots show distribution of tags in the inoculum, in cecal content of individual mice after 48h of colonization and fold increase of each tag per mouse compared to the inoculum. **(F)** Competitive index of tetracycline (Tet)- over erythromycin (Ery)-resistant strains *in vivo* after 48h of colonization in *B.theta* WT and acapsular in cecal content and in feces.

6
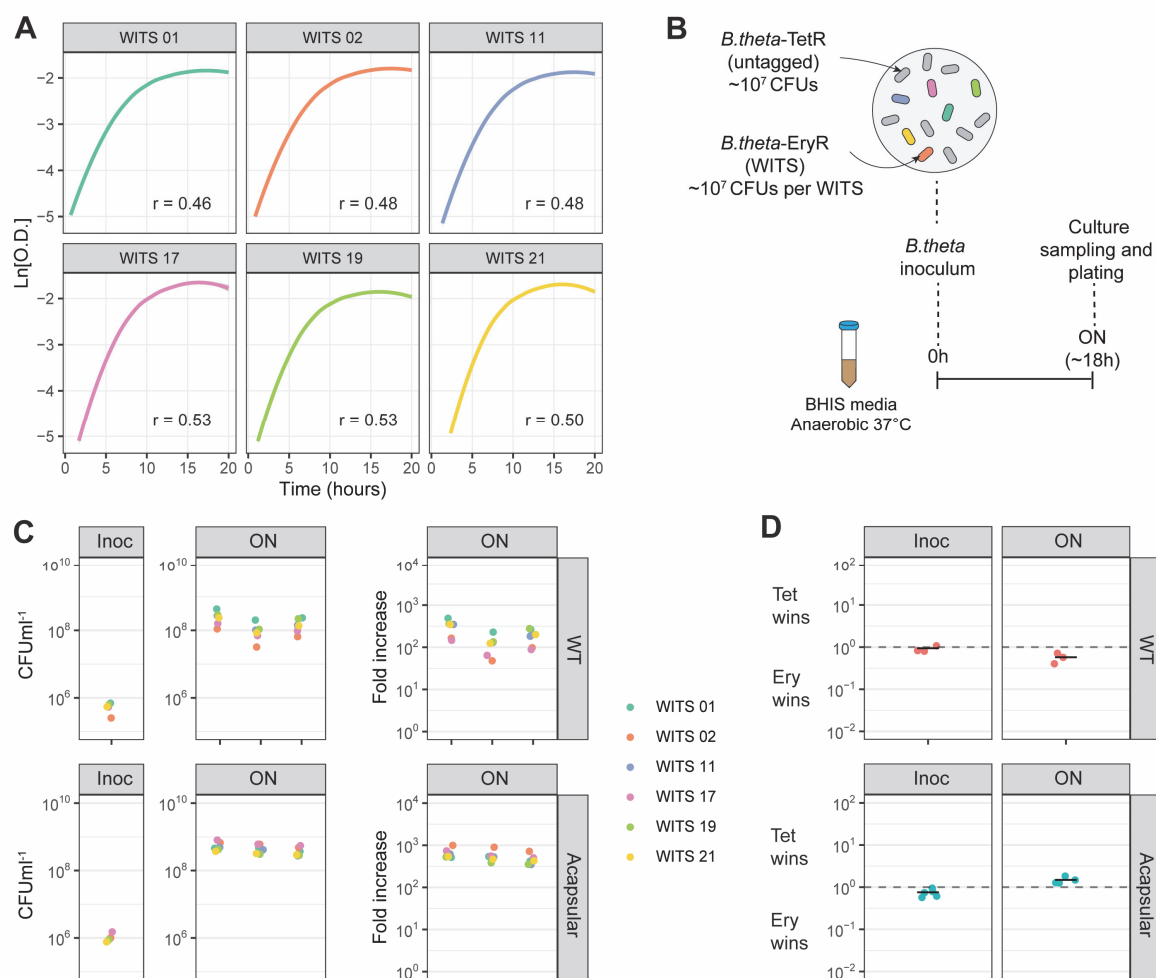
Supplementary Figure 1: Tagged *B.theta* strains have similar fitness for growing *in vitro* (A) Growth curves of *B.theta* acapsular in BHIS media and growth rates (r) per tag. **(B)** Experimental design of *in vitro* competitions. All strains (untagged *B.theta*-TetR and all six tagged *B.theta*-EryR WITS) were mixed in a 1:1 ratio. **(C)** Tags distribution after *in vitro* competition among six *B.theta* tagged strains either WT or acapsular to demonstrate neutrality *in vitro*. Plots show distribution of tags in the inoculum, in individual overnight (ON) cultures and fold increase of each tag per culture compared to the inoculum. **(D)** Competitive index of tetracycline (Tet)- over erythromycin (Ery)-resistant strains *in vitro* after ON cultures.

7

Determining inoculum size of tagged strains that yields maximal information upon *B.theta* colonization

We then applied the neutrally tagged *B. theta* strains to estimate their invasion probabilities by recovering *B. theta* cells after colonization and comparing the barcode distribution with that in the inoculum. As invasion probabilities depend on the interaction with the resident microbiota (Kurkjian et al., 2021), we probed *B.theta* colonization on three different communities: Low-complexity microbiota (LCM) (Stecher et al., 2010); Oligo Mouse Microbiota (OligoMM12) (Brugiroux et al., 2016) and specific-pathogen-free (SPF) complete microbiota (Suppl. Table 3). We evaluate recovering *B. theta* cells 48h after initial colonization, a timepoint shortly after the *B. theta* population in the cecum reaches carrying capacity (Suppl.Fig.2A).

Assuming that the change in relative abundance of tags before and after the colonization process is due to stochastic loss of *B. theta*, we formulated a mathematical model that describes this process and that allows us to infer important parameters, namely a per-cell colonization probability for *B. theta*. Mice are inoculated with n_0 copies of tagged *B.theta* cells, which undergo random killing during their transition through the stomach and small intestine. Surviving clones arriving in the cecum start growing and are detected 48h post-colonization (Fig.2A). A simple calculation was carried out to estimate the probability for the lineage of a bacterium clone spiked at n_0 copies in the inoculum to be found at the measurement time, which can be assumed as the combination of making it alive to the cecum and not being lost afterwards. As bacteria are not counted directly in the inoculum, but the inoculum is a sample of known volume of a solution of a known concentration, the incoming distribution of tagged bacteria is approximately Poisson, of mean n_0. Then we assume each bacterium has an independent probability of colonization β. Therefore, the probability of losing an individual tag (which can be approximated to the fraction of tagged strains lost across different mice) is equal to $e^{-\beta n_0}$. Finally, the colonization probability (β) can be approximated to negative natural logarithm of the proportion of lost tags divided by the expected initial number of CFUs of each tagged strain in the inoculum. As there are experiments with different initial inoculum sizes (different n_0), we obtain β by maximizing the likelihood of the experimental observations (See Methods, Mathematical modelling, section 1). Furthermore, a more complex calculation can be carried out using the variance of the tagged population rather than defined loss/retention (Suppl.Fig.2B and Suppl.Fig.2C; see Methods, Mathematical modelling, section 2), but the overall obtained numbers remain similar.

It is important to note that if all tags are lost, or if all tags are recovered, only upper or lower bounds for β can be determined, respectively, rather than numerical estimates. Thus, experiments where some, but not all tags are lost from the final population yield maximum information (Fig.2B). To find the inoculum sizes that lead to this outcome, we therefore titrated

8

138   the tagged strains into an untagged *B. theta* population at different ratios. We used these

139   mixtures to colonize mice carrying three different microbiota communities, and quantified tag

140   recovery from the cecum 48h post-colonization. We used the Pielou evenness (Pielou, 1966)

141   as a summary representation of the distributions of tagged population for both *B.theta* strains

142   (WT and acapsular) in mice carrying three different microbiota communities (Fig.2C). After an

143   analytical and numerical analysis, we found that the resulting estimates are most precise when

144   about half the tags are lost (see Supplementary Methods). In the case of LCM and OligoMM12

145   gnotobiotic mice, an n_0 of between 10-100 was optimal for both wild-type and acapsular

146   *B.theta*, whilst in SPF mice, an n_0 of around 500 was informative for wildtype, but 5000 CFU

147   were needed of each acapsular tagged strain.

148   Finally, the observed change in the distribution of tags after the colonization process can have

149   two explanations: stochastic loss of individual strains in this process, or mutation and selection

150   in a subset of the strains. In order to test whether mutations, followed by selective sweeps, can

151   explain observed changes, we recovered tagged *B. theta* strains from colonized mice, mixed

152   them with the ancestral strains carrying different tags in equal ratios, and used this mix to

153   inoculate a new group of mice. There was no consistent advantage of re-isolated strains over

154   ancestral strains (Suppl.Fig.2D), indicating that mutation and selection do not play a role in the

155   initial 48h after colonization.

9
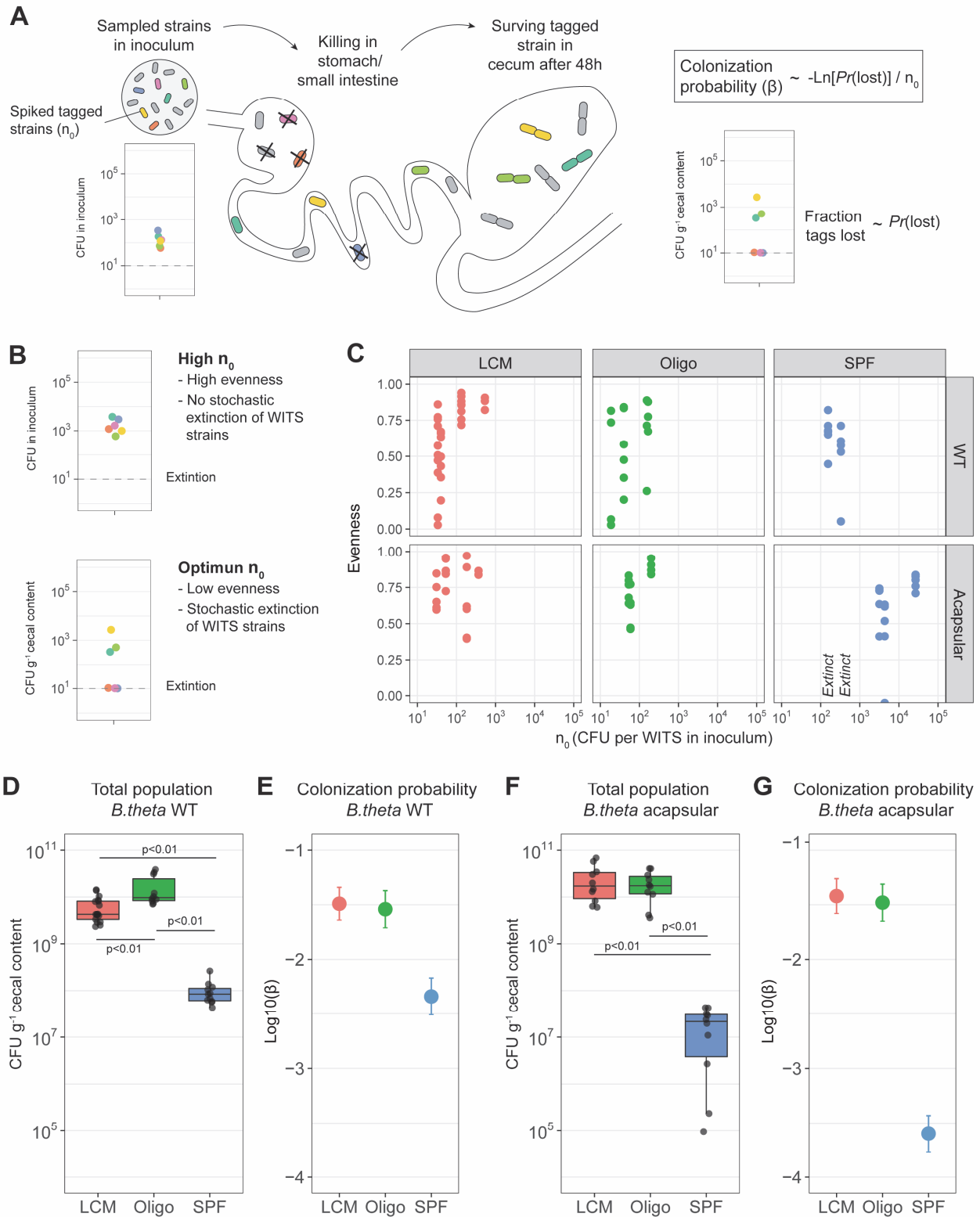
Figure 2: Colonization probability of *B.theta* strains in LCM, Oligo-MM12 and SPF mice. (A) Schematic representation of experimental estimation of colonization probability **(B)** Two different scenarios of n_0 and distribution of tagged strains: n_0 in which no extinction of tags is observed ("High n_0") and n_0 in which tags are randomly lost ("Optimal n_0"). **(C)** Pielou's evenness vs. n_0. Pielou's evenness was estimated with an maximum possible value of $H_{max} = \ln(6)$ for all data points (six tagged strains). Each dot represents the evenness calculated per mouse. Values of n_0 for which all tags were lost, and therefore no evenness could be estimated, were marked with "Extinct" in the graph. **(D and F)** Total *B.theta* population in the cecum at 48h post-colonization for **(D)** WT and **(F)** acapsular strains. **(E and G)** Probability of colonization (β) in **(E)** WT and **(G)** acapsular in the cecum after 48h of colonization using the loss method. Estimation based on 6 tags times the total number of mice (LCM=17, OligoMM12=10, SPF=11) and on lost tags.

10
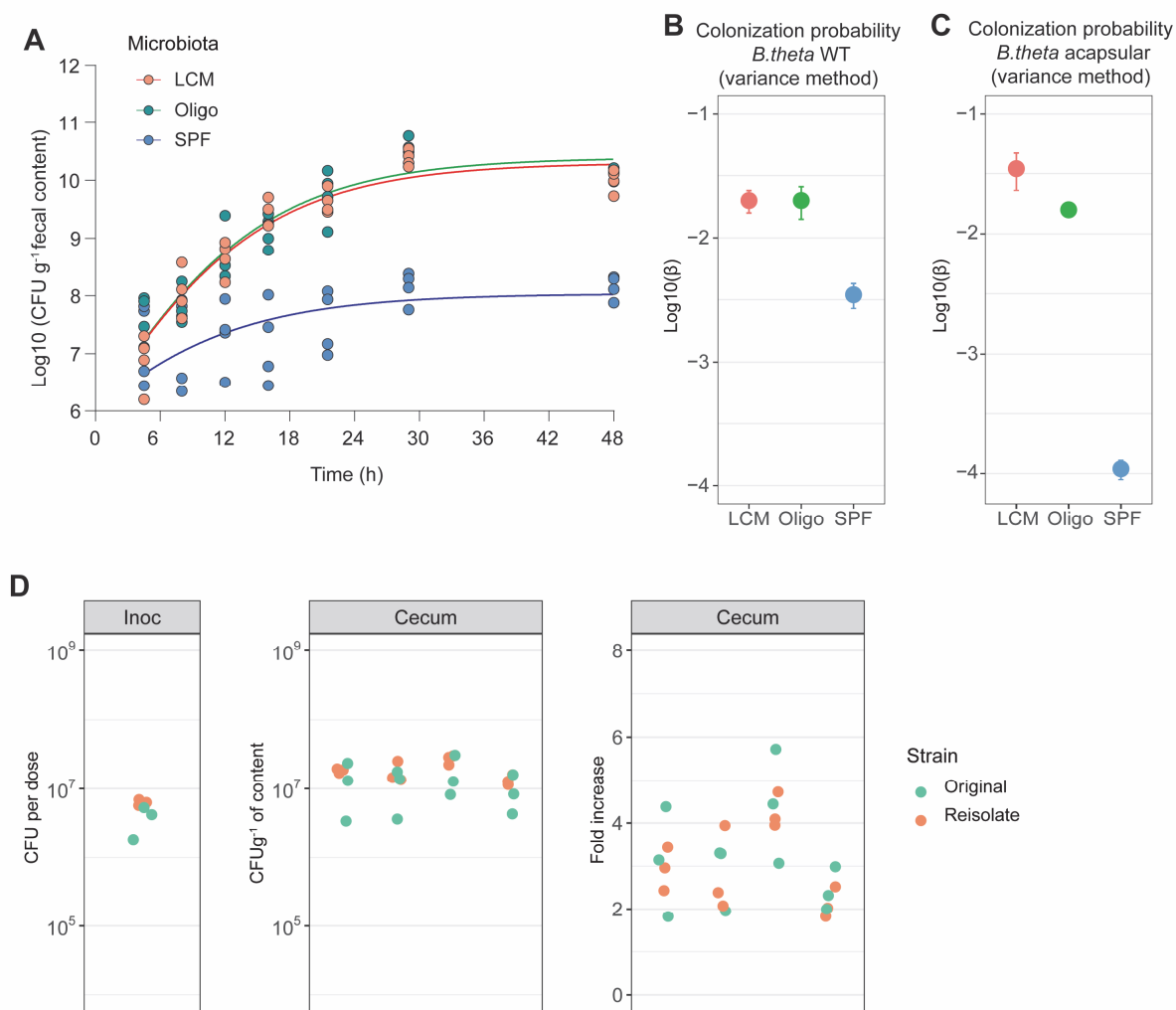
Supplementary Figure 2. (A) *In vivo* growth curve of WT *B.theta* in three different microbiota backgrounds. **(B and C)** Probability of colonization (β) for **(B)** WT and **(C)** acapsular in the cecum after 48h of colonization. Estimation based on 6 tags x m mice (LCM=17, OligoMM12=10, SPF=11) and on variance on tags before (inoculum) and after colonization (cecum). **(D)** *In vivo* competition among *B.theta* strains reisolated from SPF mice vs. original stock strains. Plots show distribution of *B.theta* original and isolated strains in the inoculum, in cecal content of individual mice after 48h of colonization and fold increase of each tag per culture compared to the inoculum.

11

156 *B.theta* colonization probability in LCM, OligoMM12 and SPF mice

157 The resident microbiota composition in the mammalian gut is one of the main factors
158 constraining the colonization of newly arriving species. This can happen through various
159 mechanisms such as competition for nutrients (Baumler and Sperandio, 2016; Maier et al.,
160 2013), modification of the intestinal environment (Cremer et al., 2017) or via direct suppression
161 of the invaders by phages (Almeida et al., 2019; Barr et al., 2013) or Type VI secretion systems
162 (Chatzidaki-Livanis et al., 2016; Wexler et al., 2016). Therefore, we used the previously
163 described mathematical model to estimate the suppressive potential of different microbiotas,
164 gnotobiotic (LCM, OligoMM12) and SPF, on *B. theta* invasion.

165 *B.theta* load in the cecal content after 48h of post-inoculation were similar in LCM and
166 OligoMM12 mice, but significantly lower in SPF mice (Fig.2D). We then used the measured
167 tag loss to determine colonization probabilities as described above, for the different *B. theta*
168 strains in the different microbiota backgrounds. The colonization probability of *B.theta* WT was
169 lower in SPF mice (Log10(β, colonization probability) ± 2 standard deviations = -2.35 ± 0.14)
170 compared to the two gnotobiotic microbiotas (LCM, -1.50 ± 0.10; and Oligo, -1.54 ± 0.13)
171 (Fig.2E). This additionally reveals that there is a discrepancy between the relative size of the
172 final population (100-fold lower in SPF mice) and the relative probability to recover a specific
173 clone from the inoculum at 48h (only 10-fold lower in SPF mice), indicating that size of the
174 open niche does not linearly translate into colonization probability. For these two observations
175 to agree, the founding population of *B.theta* has to be smaller in SPF mice, and the net growth
176 during the first 48h post-inoculation has to be lower than in the gnotobiotic mice (Suppl.Fig.2A).

177 As capsular polysaccharides (CPS) are thought to play a crucial role in phage evasion/infection
178 (Porter et al., 2020), immune evasion (Fanning et al., 2012; Hsieh et al., 2020; Porter et al.,
179 2017) and protection from other environmental stressors, we expected to see a tighter
180 bottleneck (decreased colonization probability) for the acapsular *B.theta* strain in all microbiota
181 backgrounds. Surprisingly, in gnotobiotic mice, the total population size of acapsular *B.theta*
182 and the probability to colonize (Log10β: LCM, -1.43 ± 0.13; and OligoMM12, -1.49 ± 0.14) were
183 not different to the WT strain (Fig.2F and Fig.2G). Thus, there is no measurable fitness benefit
184 of CPS in gut colonization up to 48h post-inoculation in these settings. However, we observed
185 a different scenario when we inoculated acapsular *B.theta* into mice carrying a SPF microbiota.
186 Both the total population size of acapsular *B.theta* (Fig.2F) and the colonization probability
187 (Log10β: SPF, -3.65 ± 0.13; Fig.2G) were 10-fold lower compared to the wildtype strain,
188 indicating a fitness benefit of CPS in the context of a more diverse microbiota and a smaller
189 niche. Given the previously observed absence of a growth defect for acapsular *B.theta*, we
190 hypothesized that increased clearance of acapsular *B. theta* cells causes the difference,

191 potentially attributable to competition/aggression from other microbiota species or from more
192 active host immunity in SPF mice.

193 **Competitive colonization with acapsular and WT *B.theta* reveals a role of CPS in**
194 **gnotobiotic mice**

195 The absence of an increased bottleneck during colonization of gnotobiotic mice with acapsular
196 *B.theta* is in conflict with previous studies showing a fitness defect of this strain (Coyne et al.,
197 2008; Porter et al., 2017). We therefore carried out competitive colonization with *B.theta* WT
198 and acapsular *B.theta*. Starting at a 1:1 ratio we inoculated mice with erythromycin-resistant
199 WT and tetracycline-resistant acapsular *B.theta* and quantified the cecal bacterial load 48h
200 post-inoculation (Suppl.Fig.3A). This reveals a gradient of outcompetion of the acapsular
201 strain ranging from a competitive index (abundance of WT over acapsular *B.theta* at the end
202 of the experiment) of approx. 20 in germ-free mice, 100 in gnotobiotic mice and 10^4 in SPF
203 mice (Fig.3A). This demonstrates a competitive fitness benefit of CPS, that increases in
204 proportion to microbiota complexity.

205 To confirm these findings, we performed a competition experiment in the same microbiota
206 backgrounds, but this time, using tetracycline-resistant *B.theta* WT and barcoded
207 erythromycin-resistant acapsular *B.theta* strains. WT strain density (Suppl.Fig.3B) and the
208 average increase in the WT relative to the acapsular strains (after adjusting for the initial ratio
209 in the inoculum, Suppl.Fig.3C) were similar between the two experiments. Interestingly, when
210 calculating the colonization probability *β* based on tag loss as described before, this is lower
211 for the acapsular *B. theta* strain when co-colonizing with the WT strain than when colonizing
212 alone (Fig.3B). This indicates that the competition with wild-type results in both a lower total
213 population size and increased clonal extinction in the acapsular strains.
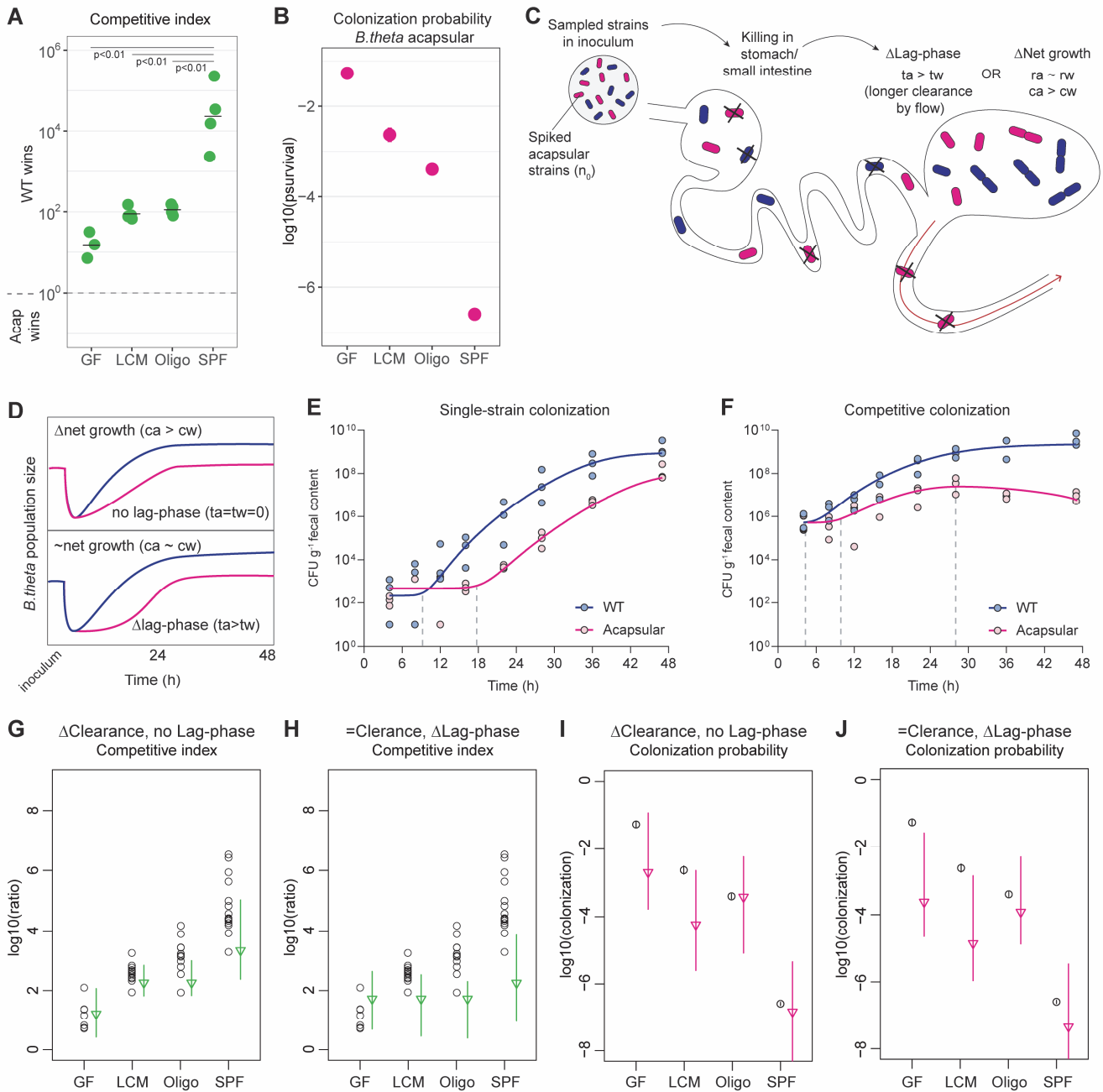
Figure 3. Competition colonization with acapsular and WT strains. (A) Competition index (ratio between WT over acapsular in the cecum) after 48h of colonization starting at a 1:1 ratio. **(B)** Probability of colonization by the acapsular strain during competition with the WT strain. Tagged acapsular strains were spiked into a WT-strain inoculum (GF=7, LCM=13, OligoMM12=12, SPF=16). **(C)** Schematic representation of two scenarios of competitive advantage of the WT over the acapsular *B.theta* having a similar initial probability of colonization of the cecum: difference in lag-phase (mean time to growth commencement in acapsular (t_a) and WT (t_w)) and difference in net growth rate (growth rate in acapsular (r_a) and WT (r_w); clearance rate in acapsular (c_a) and WT (c_w)). Clearance can be due to both flow/loss in the fecal stream and death. **(D)** Growth curves representing the two scenarios in (C). **(E)** Fecal bacterial load of *B.theta* WT or acapsular during single-strain colonization in OligoMM12 mice. Overlay graph of individual experiments with starting inoculum 10^2-10^3 CFU each. **(F)** Fecal bacterial load of *B.theta* WT or acapsular during competitive colonization in OligoMM12 mice. Overlay graph with starting inoculum 10^6 CFU each (ratio 1:1). **(G-J)** Estimation of the competitive index and colonization probability of the acapsular strain (see Supplementary Methods): **(G and I)** assuming no lag-phase and estimated difference in clearance rate between the WT and acapsular strains and **(H and J)** assuming a mean 6h difference in lag-phase and identical clearance rate between the WT and acapsular strains (circles: experimental data; triangles: mean parameter estimation and error).

14
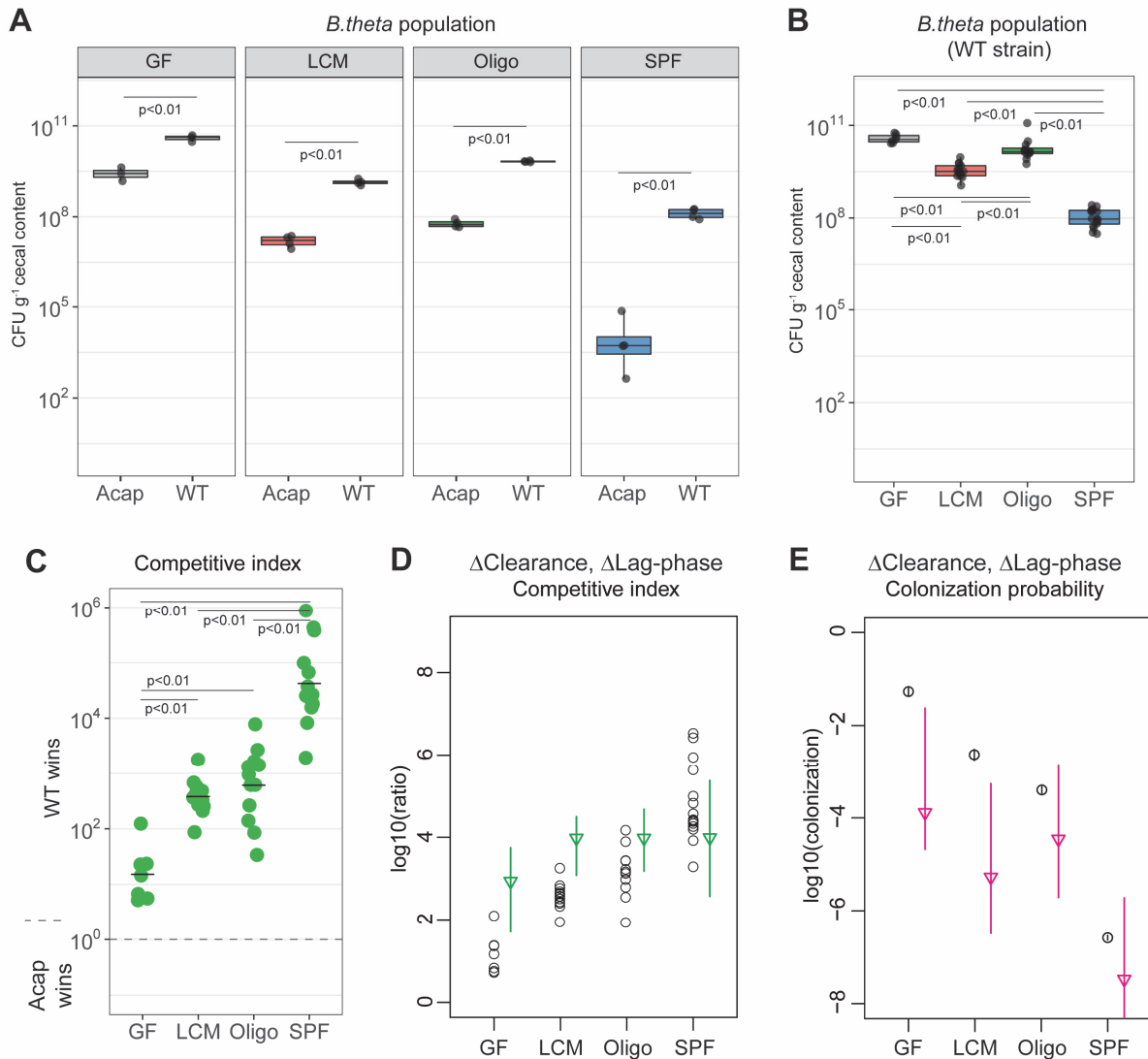
Supplementary Figure 3. (A) *C*ompetition with acapsular and WT strains during colonization starting at a 1:1 ratio. Population density of the WT and acapsular strain in cecum after 48h of colonization. **(B and C)** Estimation of probability of colonization of the cecum by the acapsular strain using a WT strain inoculum spiked with tagged acapsular strains. **(B)** Population density of the WT strain and **(C)** Competitive index after correction with the initial WT/acapsular ratio in the inoculum. **(D and E)** Estimation of the **(D)** competitive index and **(E)** colonization probability of the acapsular strain assuming a mean 6h difference in lag-phase and the estimated difference in clearance rate between the WT and acapsular strains (circles: experimental data; triangles: mean parameter estimation and error).

Longer lag-phase and higher clearance rate explains fitness defect of acapsular

***B.theta* in competitive colonization**

In order to understand how acapsular *B.theta* can have an indistinguishable colonization probability when inoculated alone, but a major fitness defect in competition with wildtype *B.theta,* we extended our simple, one-step colonization model to include a lag-phase after arrival in the cecum (Fig.3C). Based on this model, two different but non-exclusive scenarios can explain the competitive disadvantage of the acapsular strain during competition. In the first scenario, there is a difference in the net growth rate, therefore explaining the ratio between acapsular and WT strains at the end of the experiment (Fig.3D, top). In the second scenario, both strains have similar net growth rates but a different lag-time, which delays initial growth of the acapsular such that the wild-type will occupy a larger fraction of the available niche during competition (Fig.3D, bottom).

To evaluate these two different scenarios, we carried out a time-course analysis of the fecal bacterial load of *B.theta* during colonization in OligoMM12 mice for the acapsular and WT strains alone and in competition. This allows us to extract the *in vivo* net growth rates, i.e., growth rate minus clearance rate, as well as lag-phases between strains. Interestingly, the acapsular strain does exhibit an initial lag-phase of approximately 4-8h when compared to the WT, even in single colonization (Fig.3E and Fig.3F). Based on the CFU data alone, this delay in colonization could either be attributed to a tighter population bottleneck during small intestinal transit, or to a longer lag-phase of clones of the acapsular strain after arrival in the large intestine, or potentially to both. However, since our neutral tagging data indicates an identical bottleneck of wild-type and acapsular *B.theta* strains when colonized individually in OligoMM12 (Fig.2E and Fig.2G)*,* we can exclude increased killing of the acapsular strain prior to seeding of the cecum. Once in the cecum, the net growth rate during the exponential growth phase is lower for the acapsular strain (WT: 0.53±0.05 and acapsular: 0.40±0.02; estimated from Fig.3E). As the growth rates of these strains in culture is identical, it is reasonable to assume that the slightly lower net growth rate is due to an increased clearance rate for the acapsular *B.theta* in the gut lumen. This is further supported by the observed decrease in the total population of the acapsular strain after the WT has reached carrying capacity (Fig.3F).

We then use these experimentally-measured parameters to theoretically estimate the competitive index and the colonization probability of the acapsular strain during competition. We modelled three different scenarios assuming either a difference in clearance rate or lag-phase, or a combination of both (see Supplementary Methods for the description of all parameters used). Comparison of the modeled values with the observed data will then indicate whether the model can capture the dominant part of the phenomenon. We found that the competitive index (abundance of WT over acapsular strain) can be mostly explained by a

250 model in which only clearance rate differs between strains (Fig.3G). It was not possible to fit a
251 model in which only the lag-phase differed for the observed competitive index (Fig.3H). In
252 contrast, models based either on an increased clearance rate (Fig.3I) or on a prolonged lag-
253 phase (Fig.3J), could explain the observed colonization probability of the acapsular during
254 competition. Combining both parameters showed a similar tendency to the initial model without
255 a lag-phase (Suppl.Fig.3D and Suppl.Fig.3E). Therefore, while we clearly observe a delayed
256 start of growth in the acapsular strain in vivo, the increased clearance rate clearly has a
257 stronger effect on the overall abundance of the acapsular strain during competitive
258 colonization.

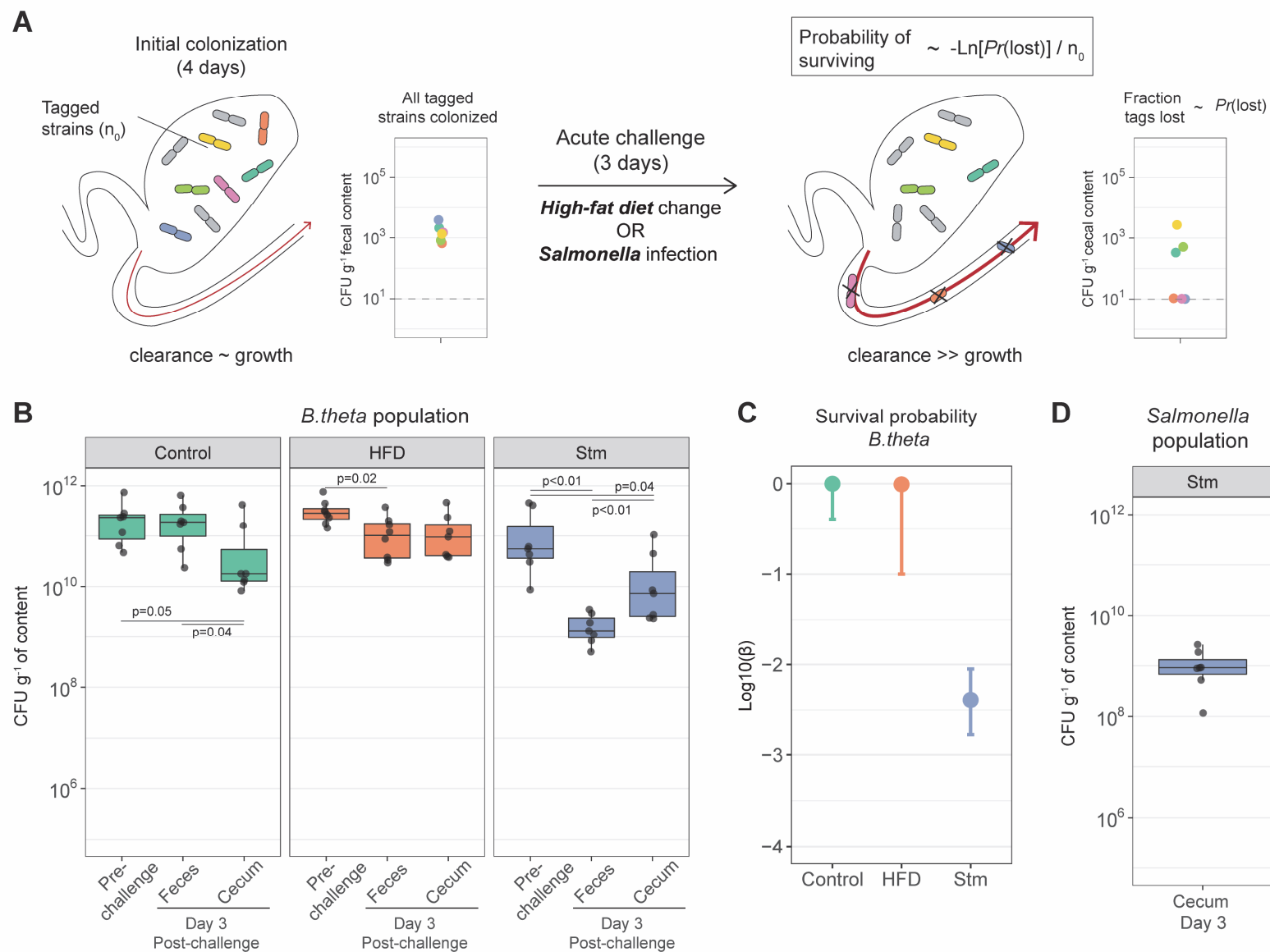### Acute challenges modify *B.theta* population dynamics in vivo

260 Finally, as a proof of concept for neutral tagging in the study of established microbiota, we
261 used our system to probe clonal extinction when an established *B.theta* population in the gut
262 is challenged by two major environmental perturbations: 1) Shifting from standard chow to a
263 high-fat no-fiber diet (HFD) (David et al., 2014; Wotzka et al., 2019)) and 2) infectious
264 inflammation driven by *Salmonella* Typhimurium (Stm) (Maier et al., 2014; Wotzka et al., 2017).

265 In order to have a highly simplified system to study host-*B.theta* interactions, we
266 monocolonized germ-free C57BL/6J mice with WT *B.theta* spiked with tagged strains in such
267 a way to maintain all tags with a roughly uniform distribution, i.e., minimum loss, in the gut
268 lumen prior to challenge (Fig.4A). After 4 days of colonization, we exposed mice to either HFD
269 or oral infection with 10^6-10^7 CFUs of attenuated Stm SL1344$^{\Delta SPI-2}$. This attenuated strain was
270 used to induce moderate intestinal inflammation in the gnotobiotic mice but to avoid the rapid
271 lethal infections associated with wildtype *Salmonella* in germ-free animals (Hapfelmeier et al.,
272 2005; Stecher et al., 2005). *B.theta* populations were monitored in feces before the challenge
273 was administered and three days after the challenge in feces and cecum.

274 Despite published reports that *B.theta* is sensitive to bile acids (Wotzka et al., 2019), HFD did
275 not significantly change the cecum population size (Fig.4B) or increased loss of tagged *B.theta*
276 (Fig.4C) in the diet-shift experiments. We can still set a lower-bound for the probability of an
277 established *B.theta* clone to survive the acute dietary challenge by estimating the value in case
278 that one tagged strain was lost during the challenge. In this case, HFD imposed a similar
279 survival probability ($Log10(\beta)$ = -1 to 0) to the one observed in the control group ($Log10(\beta)$ = -
280 0.39 to 0). Estimating that the initial *B.theta* population is in the order of 10^{10} CFUg^{-1} in the
281 cecum, the bottleneck effect imposed by HFD would reduce the population minimally to a range
282 between 10^9 to 10^{10} clones, which are densities normally observed in the cecum (Fig.4B).

283 In contrast, after three days of infection, *Salmonella* induced-inflammation reduced the total
284 *B.theta* population approx. 100-fold in feces at day 3 post-infection (Fig.4B). In addition, we

17

285   estimated the probability of an established clone to survive this acute inflammation challenge

286   is approximately 1 out of 500 in cecum (Fig.4C) while competing with the *Salmonella*

287   population (Fig.4D). This means that the initial estimated population of 10^{10} CFUg^{-1} in the

288   cecum is reduced to a population of between 10^7 to 10^8 clones by the bottleneck effect induced

289   by inflammation and then bouncing back to the observed levels between 10^9 to 10^{10} CFUg^{-1}

290   (Fig.4B). Therefore, the bottleneck effect on the population induced by acute inflammation not

291   only reduces the total population size but also diminishes the diversity of clones in the

292   population.

Figure 4. Acute challenges imposed a population bottleneck in the resident *B.theta* population. (A) Schematic representation of experimental estimation of colonization survival probability after acute challenges. **(B)** Population of *B.theta* in monocolonized ex-GF mice kept under standard chow (control) and during acute challenge with high-fat diet (HFD) or attenuated *Salmonella* infection. **(C)** Probability of surviving in the cecum after 3 days of the acute challenge. Estimation based on 6 tags timer the total number of mice (Control=7, HFD=8, Stm=7). **(D)** Population of attenuated Salmonella in cecal content.

Discussion

Understanding the different mechanistic factors determining how microbes can invade a resident gut microbiota is of considerable importance for combating mucosal infections (Kreuzer and Hardt, 2020; Stecher, 2021), but also for rationally introducing new functions into existing communities (Cubillos-Ruiz et al., 2021). These factors can include, among others, nutrient/energy availability, environmental factors such as pH and flow/dilution rate (Arnoldini et al., 2018), and the presence of directly toxic or aggressive activities derived from the host (Cullen et al., 2015) or from other microbiota species (García-Bayona and Comstock, 2018), all of which can affect different microbes in different ways. Here, we condense all these mechanisms into three processes: factors affecting immigration rate (i.e., arrival into growth-permissive sites in the gut), factors affecting growth, and factors affecting clearance/death (Hoces et al 2020). Combining well-designed experiments using genetically barcoded strains with mathematical modeling, we were able to empirically (e.g., net growth rates through plating) or deductively (e.g., probability of colonization) estimate the relative importance of these three processes for colonization of *B. theta* under different conditions. In addition, we were able to study mechanistically how fitness-relevant genetic changes in *B. theta* (production of capsular polysaccharide) affect colonization success.

When analyzing the effect of capsular polysaccharide expression in the process of colonizing mice with different resident microbiotas, we found that the previously shown fitness disadvantage of acapsular strains (Coyne et al., 2008; Porter et al., 2017) depends on the microbiota context, rather than on host effects. Both, the wild type and the acapsular strains colonize mice with a relatively simple microbiota (LCM, Oligo) similarly well. However, in mice with more complex microbiota (SPF), the acapsular strain engrafted significantly less well than the wild type. While a possible explanation includes more robust intestinal immunity in fully colonized SPF mice, the simplest explanation is that expression of CPS is primarily important for interaction with or protection against other microbes. Possible microbe-inflicted processes against which CPS can protect include microbe-on-microbe killing (Chatzidaki-Livanis et al., 2016; Wexler et al., 2016) and susceptibility to phages (De Sordi et al., 2019; Porter et al., 2020). Co-colonization experiments with mixed *B. theta* inoculums consisting of wild type and acapsular strains revealed the specific disadvantages of the acapsular strain: a longer lag-phase before it starts growing in the gut and a higher clearance rate.

The effect of two important challenges with known effects on resident commensals, high-fat feeding (Wotzka et al, 2019) and inflammation (Maier et al, 2014), differentially affect *B. theta* and seem to depend on the ecological context in different ways. Feeding mice which are stably monocolonized with *B. theta* a fiber-less high-fat diet imposes a surprisingly mild bottleneck on the *B. theta* population 3 days after treatment, even though this intervention has been shown

329   to increase bile acid concentrations to levels that inhibit *B. theta* growth (Wotzka et al, 2019).

330   As it has been shown that *B.theta* rapidly evolves to adapt to dietary challenges in the context

331   of a resident microbiota (Dapa et al., 2022), the observed mild population bottleneck imposed

332   by high-fat diet feeding might only manifest if *B. theta* competes against other gut microbiota

333   members, potentially ones that are more resistant to bile salts (e.g., *E. coli*, see Wotzka et al,

334   2019). When infecting mice that are stably monocolonized with *B. theta* with Salmonella, we

335   observed a larger decrease in *B. theta* clonal survival probability, which is consistent with the

336   sensitivity of commensal species to gut inflammation (cite Stecher et al, 2007). Interestingly,

337   inflammation also causes a population bottleneck in the infecting *Salmonella* population (Maier

338   et al, 2014), but it is less pronounced than the one we observe for *B. theta*, and the total

339   population size of *Salmonella* rapidly recovers after this bottleneck. Therefore, the rapid

340   killing/clearance of gut luminal *B. theta* seems to be representative of microbiota suppression

341   that underlies the loss of colonization resistance observed in Salmonella-induced colitis.

342   Of course, our mathematical models are based on certain assumptions which are useful to

343   simplify calculations but always risk introducing bias. Most notably, we have made estimates

344   for a single population of bacteria that has a constant growth and clearance rate. Necessarily

345   the reality is more complex than this – the nutrient profile and motility of the intestine will vary

346   with circadian rhythm. Also previous work has demonstrated that particular CPS-expressing

347   clones may have an advantage colonizing the mucus (Donaldson et al., 2018), although

348   gnotobiotic studies suggest that at the population level *B.theta* grows at a similar rate in the

349   mucus layer and lumen (Li et al., 2015). Nevertheless, recognizing these limitations, our

350   estimates of colonization probability, growth and clearance rates still give a good overview of

351   the harsh processes with strong effects on the *total* intestinal *B.theta* population. Future works

352   should include individual-based models that can evaluate the impact of bacterial clones with

353   different distributions of growth/clearance rates, as well as working with experimental models

354   (microfluidics, for example) that would allow experimental investigation of the impact of single-

355   cell level variation on total population behavior.

356   By combining mathematical modelling with direct quantification of bacterial population

357   dynamics, we can gain insight into the major phenomena influencing colonization efficiency.

358   Not only do these results help us understand the different steps of *B. theta* colonization, but

359   they also serve as a proof of concept for studying other complex, multi-step biological

360   processes using the set of experimental and data-analysis tools we are describing here. This

361   raises the possibility to optimize colonization conditions in order to promote the efficient

362   engraftment of beneficial species into target microbiota, or to better understand the processes

363   of invasion of pathogens and the functional basis of colonization resistance.

Acknowledgements

Funding

Author Contributions

Conceptualization, D.H., M.A., C.L. and E.S.; Methodology, D.H., G.G., M.A., I.K., F.B., A.W., E.M., C.L. and E.S.; Formal Analysis, D.H., M.A., C.L., and E.S.; Investigation, D.H., G.G., C.M., S.B., C.L.; Resources, I.K., J.H., E.M., W-D.H., C.L. and E.S.; Writing – Original draft, D.H. and E.S.; Writing – Review and Editing D.H., G.G., M.A., C.M., S.B., I.K., F.B., A.W., J.H., E.M., W-D.H., C.L. and E.S.; Visualization, D.H., M.A., C.L. and E.S.; Supervision, C.L. and E.S.; Funding acquisition, C.L. and E.S.

Declaration of Interest

The authors declare no competing interests.

Methods

Bacterial strains and cultures

B. theta strains were grown anaerobically (5%H_2, 10%CO_2, rest N_2) at 37°C, overnight in brain heart infusion (BHI) supplemented media (BHIS: 37g/L BHI (Sigma); 1g/L-cysteine (Sigma); 1mg/L Hemin (Sigma)). For enrichment cultures in plates, we used BHI-blood agar plates (37g/L BHI (Sigma); 1g/L-cysteine (Sigma); 10% v/v defibrinated sheep blood (Sigma)). Antibiotics were added to liquid cultures or plates as required for strain selection: erythromycin 25µg/L or tetracycline 2µg/L. In the case of BHI-blood agar plates used for cloning or gut content enrichment, we additionally added gentamycin 200µg/L to all plates. Plates were incubated for 48-72h at 37°C in anaerobic conditions. For a complete list of the bacterial strains used in this study, see Suppl. Table 1.

Isogenic tag construction and integration

Genetic tags, fluorescent proteins and antibiotic resistance were introduced by using the mobilizable *Bacteroides* element NBU2, which integrates into the *Bacteroides* genomes at a conserved location (Wang et al., 2000). Gene fragments containing a unique 40bp sequence (biding site for forward primer) and a 609bp sequence with the ydgA pseudogene (common binding site for reverse primer) were synthesized (gBlocks, Integrated DNA Technologies) and cloned by Gibson Assembly Master Mix (NEB) into an NBU2 plasmid carrying the erythromycin resistant cassette ermG (tagged *B.theta*-EryR strains). A similar NBU2 plasmid carrying the tetracycline resistant cassette tetQb was used to construct the untagged strains (*B.theta*-TetR). For both, we used 10µL of desalted assembly reaction products to transform competent *E.coli* S17-1 cells (mid-log cells, washed three times in deionized ice-cold water) by electroporation (V=1.8kV; MicroPulser, BioRad). After 1h recovery at 37°C in 1mL of LB, cells were plated on LB plates with chloramphenicol (12µg/mL) and grown overnight. Plasmid-carrying *E.coli* S17-1 and *B.theta* strains were cultured overnight in 5mL of liquid media. *E.coli* S17-1 and *B.theta* were washed with PBS, pooled in 1mL of PBS, plated BHI-blood agar plates without antibiotics, and grown aerobically at 37°C for at least 16 hours. The lawn of *E.coli* S17-1 and *B.theta* was collected in 5mL of PBS, homogenized by vortex and 100µL were plated in BHI-blood agar plates supplemented with erythromycin 25µg/L and gentamycin 200µg/L. After 48 hours, single colonies were streaked in fresh BHI-blood agar plates with antibiotics, to avoid potential contamination with WT strains. Successful insertion in the BTt70 or BTt71 sites was evaluated by PCR.

In vitro growth curves and competition

Individual *B.theta* strains were grown overnight on BHIS. Stationary-phase cultures were washed with PBS, and O.D. was quantified and adjusted to 0.05 in 200µL of fresh BHIS in a round 96-well tissue culture plates. Plates were transferred into the anaerobic tent and growth was quantified at 37°C with shaking, using a plate reader (Infinite PRO 200, Tecan).

For competition experiments, stationary-phase cultures *B.theta* WT or acapsular strains were washed with PBS, O.D. was quantified and adjusted to approximately 5×10^6 CFU/mL per strain (one *B.theta*-TetR and six *B.theta*-EryR tagged strains) in 10mL of fresh BHIS. An aliquot of this mix was serially diluted and plated in BHI-blood agar plates with the respective antibiotics for CFU quantification. Cultures were kept overnight, with shaking (800rpm) at 37°C in the anaerobic tent. Afterwards, an aliquot was plated as described before. For assessing the competition between *B.theta* tagged strains, we isolated DNA from one of the dilutions used for quantification and assessed the relative distribution of the tags by qPCR (see Quantitative PCR section). For assessing the competition among strains with different antibiotic resistances, we calculated the competition index by dividing the CFU/mL of the untagged *B.theta*-TetR strain (tetracycline-resistant) by the adjusted number of *B.theta*-EryR tagged strains (erythromycin-resistant; CFU/mL divided by six, as all the tagged strains were present in the culture).

Mice

All animal experiments were performed with approval from the Zürich Cantonal Authority. In all experiments, we used mice with C57BL/6J genetic background, between 12-15 weeks old and of variable gender. C57BL/6J germ-free and gnotobiotic mouse lines (Low-complexity microbiota (LCM) (Stecher et al., 2010); Oligo Mouse Microbiota (OligoMM12) (Brugiroux et al., 2016)) were raised in surgical isolators under high hygiene standards at the ETH Phenomic Center. C57BL/6J SPF mouse line was also raised in the same facility. Mice were transferred to our experimental facility in sterile, tight closed cages and house into the IsoCage P-Bioexclusion System (Tecniplast) for 24h-48h before the experiment to adapt to new housing conditions. In all experiments, standard chow and water was supplemented under strict sterile conditions to avoid potential contaminations.

In vivo growth curves and competition

B.theta WT WITS 01 strain was grown overnight on BHIS. Stationary-phase cultures were washed with PBS, and an inoculum of ~5×10^7 CFUs/100µL dose was prepared. C57BL/6J mice carrying the described microbiota composition (LCM, OligoMM12, SPF, 4 mice per group) were gavaged with the inoculum and fecal pellets were collected approximately every 4h for the first 20h, followed by two extra time points at 29h and 48h post-inoculation. Fecal pellets

456   were weighted and homogenized in 500µLof PBS with steel ball by mixing (25Hz, 2.5min) in a

457   TissueLyser (Qiagen). Serial dilutions were plated for quantification on BHI-blood agar plates

458   supplemented with gentamycin 200µg/L and erythromycin 25µg/L.

459   For competition experiments, *B.theta* strains were grown overnight in 8mL of BHIS with

460   corresponding antibiotics (erythromycin 25µg/L or tetracycline 2µg/L). Each culture was spun

461   down at 3000g for 20min and resuspended in 10mL of PBS and individual O.D. was measured

462   (cell number estimation 1 O.D.=~$4x10^8$ cells/mL). Each strain was adjusted to approximately

463   $5x10^6$ CFU/100µL dose per strain in the inoculum mix (one *B.theta*-TetR and six *B.theta*-EryR

464   tagged strains). Germ-free mice were gavaged with 100µL of the inoculum. After 48h, fecal

465   and cecal contents were collected. Fecal content was homogenized and plated for

466   quantification as described before. Cecal content was resuspended in 1mL of PBS and

467   homogenized with steel ball by mixing with the same protocol (25Hz, 2.5min). Serial dilutions

468   were prepared and plated in BHI-blood agar plates supplemented with gentamycin plus either

469   erythromycin or tetracycline for CFU quantification of each strain. Similar to the in vitro

470   competition experiment, we isolated DNA from one of the dilutions used for quantification to

471   assess the competition between *B.theta* tagged strains. Relative distribution of the tags was

472   obtained by qPCR. For calculating the competition index among strains with different antibiotic

473   resistances, we divided the bacteria density of the untagged *B.theta*-TetR strain by a sixth of

474   the bacteria density of the total *B.theta*-EryR tagged strains (as all six tagged strains were

475   present in the culture).

Colonization experiments

477   Stationary-phase *B.theta* strains were grown overnight as described before. Each culture was

478   washed once with PBS and adjusted in the inoculum based on its O.D. For the untagged strain

479   (*B.theta*-TetR), ~$5x10^7$ CFUs/100µL dose were transferred to the inoculum. For the *B.theta*-

480   EryR tagged strains, we prepared an initial mix of all tagged strains in 50mL of PBS to a

481   concentration of 10^5 CFU/mL of each strain. After mixing by vortex for 1min, the required

482   amount of *B.theta*-EryR tagged strains was spiked into the inoculum (between 30 - $5x10^4$ CFUs

483   depending on the experiment). Gnotobiotic (LCM, Oligo) and SPF C57BL/6J mice were

484   gavaged with the 100µL inoculum. Inoculum was serially diluted and plated for quantification

485   of CFUs in BHI-blood agar plates supplemented with gentamycin 200µg/L plus either

486   erythromycin 25µg/L or tetracycline 2µg/L. In addition, 2-3 doses (100µL) were directly plated

487   in BHI-blood agar plates with gentamycin plus erythromycin to address initial distribution of

488   *B.theta*-EryR tagged strains in the inoculum by quantitative PCR (qPCR). Two days after

489   colonization, mice were euthanized and cecal content was collected in 2mL Eppendorf tubes

490   and weighted. Cecal content was homogenized as described before. Serial dilutions were

491   prepared and plated in BHI-blood agar plates supplemented gentamycin plus either

25

492   erythromycin or tetracycline for CFU quantification. In addition, 100μL of homogenized content

493   was plated directly in BHI-blood agar plates with gentamycin plus erythromycin for further

494   assessment of the distribution of *B.theta*-EryR tagged strains by qPCR.

495   **In vivo competition of post-colonization versus original strains**

496   To discard potential increased colonization fitness in the tagged strains that were present in

497   the cecum content after 48h, we isolated single *B.theta* WT tagged strains that were present

498   in the cecal content of SPF during a colonization experiment. Single colonies were expanded

499   in liquid media, and the presence of a single strain was confirmed by qPCR analysis of the

500   tagged tag. We randomly selected three of the *B.theta* WT tagged strains isolated from the

501   cecal content. We prepared an inoculum as described before for the in vivo competition

502   experiments with approximately 5×10^6 CFU/100μL dose per strain in the inoculum mix. We

503   complemented the inoculum with the remaining three *B.theta* WT tagged strains coming from

504   the original stock. SPF mice were inoculated by gavage and cecal content was collected 48h

505   later. Cecal content was processed as described before for CFU quantification and relative tag

506   distribution by qPCR.

507   **Diet modification and Infection challenge experiments**

508   In accordance with what we described before, *B.theta* WT strains were grown overnight in

509   BHIS with corresponding antibiotics. As the untagged strain *B.theta*-TetR was used in higher

510   concentrations, we prepared between 50-100mL of liquid culture depending on the number of

511   mice to colonize. Inoculum was prepared as previously described with a concentration of 10^8-

512   10^9 CFUs/100μL dose of untagged *B.theta*-TetR, spiked with approximately 30 CFU of each

513   *B.theta*-EryR tagged strains. Germ-free mice were gavaged with 100μL of the inoculum. Mice

514   were maintained on standard chow diet (Kliba Nafag, 3537; autoclaved; per weight: 4.5% fat,

515   18.5% protein, ~50% carbohydrates, 4.5% fiber) for 4 days. Afterwards, mice were housed on

516   fresh IsoCages and challenges were applied as follows: 1) Control group (continuation of

517   standard chow diet); 2) Western-type diet without fiber (BioServ, S3282; 60% kcal fat;

518   irradiated; per weight: 36% fat, 20.5% protein, 35.7% carbohydrates, 0% fiber); or 3) infection

519   with 5×10^7 CFU of attenuated *Salmonella* Typhimurium (Stm SL1344$^{\Delta SPI-2}$). Fecal pellets were

520   collected pre-challenge (day 0) and during the following three day. On the day 3, mice were

521   euthanized and cecal content was collected. Fecal pellets were weighted and homogenized in

522   500μLof PBS as described before. Serial dilutions were prepared and plated in BHI-blood agar

523   plates supplemented with corresponding antibiotics for CFU quantification. In addition, 100-

524   300μL of homogenized content was plated directly for further assessment of the distribution of

525   *B.theta*-EryR tagged strains by qPCR. Cecal content was processed as previously described.

Quantitative PCR

Colonies from enrichment plates were pooled in 5ml of PBS and homogenized by vortex. Genomic DNA was isolated with the QIAamp DNA Mini Kit (Qiagen). qPCR was performed using with FastStart Universal SYBR Green Master Mix (Roche, Cat. N° 4385610). Primers (Supplementary Table 2) were mixed to a final concentration of 1µM. Between 160-200ng of DNA was amplified using StepOne Plus or QuantStudio 7 Flex instruments (Applied Biosystems) using the following protocol: initial denaturation at 95°C for 14min followed by 40 cycles of 94°C for 15sec, 61°C for 30sec, and 72°C for 20sec as described previously.

Mathematical modelling

1. Estimation of colonization probability based on lost tags

Let us denote C the bacterial concentration in the prepared solution. Then, if there is a volume V of solution, then there are $N = CV$ bacteria. Therefore, the probability to have taken n_0 bacteria in a volume v_0 is:

$$p(n_0) = Binomial\ distribution(N, n_0/V) = \left(\frac{v_0}{V}\right)^n \left(1 - \frac{v_0}{V}\right)^{N-n_0} \frac{N!}{(N-n_0)! n_0!} \qquad (1)$$

In the limit of $N = cV$ large and $v_0 \ll V$,

$$p(n_0) \cong Poisson\ distribution(N\ v_0/V) = \frac{(Nv_0/V)^{n_0} \exp(-Nv_0/V)}{n_0!} \qquad (2)$$

Let us define β as the probability for each bacterium to get to the cecum alive, and then have its lineage survive until measurement. There are a priori no interactions early on between incoming bacteria, as their concentration is initially low enough to limit the competition between them before arriving to the cecum. Then, the probability for a tagged *B.theta* strain not to be present at measurement time, if started with an average of n_0 bacteria (Poisson distributed) is the zero of the Poisson distribution of average βn_0, and thus:

$$p_{loss} = \exp(-\beta n_0) \qquad (3)$$

As n_0 is estimated via the concentration and volume of the inoculum, and p_{loss} is best estimated via the number of tags lost divided by the total number of tags, then β is estimated as:

$$\beta \cong \frac{-log(n_{loss\ tags}/n_{tags})}{n_0} \qquad (4)$$

To consider the fact that not all tags have the same n_0, β is actually estimated by its value maximizing the probability of the experimental observations, thus β maximizing:

$$LL = \sum_{i=1}^{\omega} \log\left((\exp(-\beta n_i))^{l_i} (1 - \exp(-\beta n_i))^{1-l_i}\right) \qquad (5)$$

555 This expression is also used for calculating the confidence interval, as detailed in appendix.

556   *2. Estimation of colonization probability based on variance*

557 The variance on the proportions is:

558
$$var(p) = \frac{1}{h_1}\sum(p_i - \frac{1}{h})^2 = \frac{1}{h_1}\sum(\frac{n_i}{\sum n_j} - \frac{1}{h})^2 \qquad (6)$$

559 In the limit where the initial number of bacteria are of the same order of magnitude, we find:

560
$$\langle var(p)\rangle - var(p_0) \cong \frac{1}{h\sum n_{j,0}}\frac{var1}{m1^2} \qquad (7)$$

561 with $var(p_0)$ the variance in proportions in the inoculum, $\sum n_{j,0}$ the total number of tags in the
562 inoculum, and $var1/m1^2$ the relative variance starting from one bacterium. We find (see
563 Supplementary Methods) that $var1/m1^2$ is 2/(colonization probability). Then $var1/m1^2$ is
564 estimated for each mouse using equation (7), and the average variance is used to estimate
565 $var1/m1^2$. The standard error on $var1/m1^2$ is used to obtain the confidence interval for the
566 colonization probability.

567   *3. Estimation of clearance rate due to flow*

568 We examined the expected magnitude of the effect of an extended lag phase in the cecum on
569 colonization probability to determine whether this is consistent with our observed neutral
570 tagging data. It should also be noted that the cecum is a dynamic environment with pulsatile
571 arrival of material from the small intestine and loss of material to the feces. This generates a
572 clearance rate due to flow, on top of any clearance rate due to bacterial death. Assuming that
573 the main site of growth of *B.theta* is the cecum/upper colon, the parameter for clearance due
574 to flow can be estimated by quantifying the volume of cecum content lost per day. This can be
575 empirically estimated by measuring 1) fecal dry mass produced per day, and 2) the water
576 content of cecum content. Assuming minimal change in dry mass during colon transit in the
577 mice, this infers a dilution rate of cecal content in the order of 0.12 volumes/h in a germ-free
578 mouse and 0.18 volumes/h in an SPF mouse; gnotobiotic mice will have a value in between
579 these two. Bacterial clearance due to killing will contribute over and above these values. Of
580 note, bacteria with a long lag-phase after introduction into the cecum will be cleared by the
581 flow before growth can start, i.e., during the early phase of colonization this will be a
582 determinant of colonization probability.

Estimation of cecum turnover rates

	Water fraction in	Dry fecal excretion (gram/day)	Estimated wet cecal mass	Wet cecal mass (gram)	Estimated cecum	Estimated cecum

	cecal mass (%)		excretion (gram/day)		turnover rate (volume/day)	turnover rate (volume/h)
Germ-free	80.9 (0.4)	1.55 (0.27)	8.12 (1.42)	2.83 (0.59)	2.87 (0.78)	0.12 (0.03)
SPF	76.2 (1.2)	0.81 (0.09)	3.40 (0.42)	0.77 (0.32)	4.42 (1.91)	0.18 (0.08)

583   *4. Estimation of the competitive index*

584   We assume that bacteria have first a probability of survival q_i (with $i = w$ for the WT strain, and

585     $i = a$ for the acapsular strain). Then once the cecum is reached, they have a loss rate c_i.

586   During an initial lag-phase τ_i, they do not grow. Then, each bacterial strain grows logistically,

587   initially at a rate r_i, which saturates when approaching carrying capacity with a factor $(1 - (A +$

588     $W)/K)$. When carrying capacity is reached, the total number of bacteria remains constant until

589   the end of the experiment at time t_{tot}, with both loss and replication ongoing and compensating

590   each other. Given the growth rates for WT and acapsular are similar in vitro, we assume $r_w =$

591   r_a, so that the difference in the initial net growth rates $(r_i - c_i)$ originates from $c_a > c_w$.

592   Therefore, in the competition setting, the population is mostly composed of WT when carrying

593   capacity is reached, so that the global population size is depleted with rate approximately c_w.

594   As a result, the effective residual replication rate of both types exactly compensates the loss

595   rate, c_w, because they compete for the same resources and have the same growth ability. As

596   acapsular keep being lost at a larger rate ca, their net growth rate at carrying capacity is

597   negative, so that they keep decreasing in frequency in the population.

598   With this model (see detailed calculations in Supplementary Methods), we find that the relative

599   ratio between WT and acapsular is:

600           $$\frac{q_\omega}{q_a} exp((net_w + c_\omega)(\tau_a - \tau_w))(\exp((net_w - net_a)t_{tot})) \qquad (8)$$

601   For all the microbiota except SPF, as the colonization probabilities were similar for the WT and

602   acapsular, then we assume $q_a = q_w$. For SPF, we use the ratio of q_w / q_a in the colonization

603   experiments, adjusted for the fact that the full colonization probability also includes steps after

604   the initial death before reaching the cecum.

605   All the parameters used are determined using experiments other than the competition

606   experiment (except for t_{tot}, the total experimental time).

607   *5. Estimation of colonization probability during competition*

608   We find that the overall survival probability for the acapsular in the competition experiment is

609   the colonization probability from the colonization experiment (alone), multiplied by a factor

610 considering later loss (when the carrying capacity is reached by the WT and the acapsular

611 decreases). The complete expression can be found in the corresponding section of the

612 Supplementary Methods.

613 *6. Estimation of survival probability after challenge*

614 In these experiments, at the time of the start of the challenge, the bacterial population is at

615 carrying capacity, so the effective growth rate (likely limited by availability of nutrients) is about

616 the same as the loss rate. Also, let us assume that the population the population size is known

617 at this time. Then, a challenge is applied. A challenge may have different effects: it may impose

618 a temporary bottleneck in the population (loss becomes higher than reproduction), or it may

619 increase the loss rate (with the reproduction rate increasing enough to compensate), and thus

620 the turnover of the population. In any case, we can calculate β as the probability that a bacteria

621 present at day=0 of the challenge has its lineage still alive at day 3. Then, if there are n_0

622 bacteria of a given type at day=0, then:

$$p_{loss} = (1 - \beta)^{n_0} \qquad (6)$$

624 To estimate the total population size in the cecum at before the challenge (n_0), we assume

625 that (1) all the animals are in the control conditions at day=0, and (2) the cecum mass and

626 bacteria concentration is the same on day=0 and day=3 in the control group. Therefore, the

627 average ratio of the concentration of bacteria in feces relative to cecum at day=3 in the control

628 animals is used to estimate the bacterial concentration in the cecum at day=0. Then, we

629 estimate the proportion of each tag strain in from the total tagged-bacteria CFU counts using

630 the relative distribution the qPCR data. In addition, p_{loss} is best estimated via the number of

631 tags lost divided by the total number of tags.

References

Abel S, Abel Zur Wiesch P, Chang HH, Davis BM, Lipsitch M, Waldor MK. 2015a. Sequence tag-based analysis of microbial population dynamics. *Nat Methods* **12**:223–226. doi:10.1038/nmeth.3253

Abel S, Abel zur Wiesch P, Davis BM, Waldor MK. 2015b. Analysis of Bottlenecks in Experimental Models of Infection. *PLOS Pathog* **11**:e1004823. doi:10.1371/journal.ppat.1004823

Almeida GMF, Laanto E, Ashrafi R, Sundberg LR. 2019. Bacteriophage adherence to mucus mediates preventive protection against pathogenic bacteria. *MBio* **10**. doi:10.1128/mBio.01984-19

Arnoldini M, Cremer J, Hwa T. 2018. Bacterial growth, flow, and mixing shape human gut microbiota density and composition. *Gut Microbes* 1–8. doi:10.1080/19490976.2018.1448741

Barr JJ, Auro R, Furlan M, Whiteson KL, Erb ML, Pogliano J, Stotland A, Wolkowicz R, Cutting AS, Doran KS, Salamon P, Youle M, Rohwer F. 2013. Bacteriophage adhering to mucus provide a non-host-derived immunity. *Proc Natl Acad Sci U S A* **110**:10771–10776. doi:10.1073/pnas.1305923110

Baumler AJ, Sperandio V. 2016. Interactions between the microbiota and pathogenic bacteria in the gut. *Nature* **535**:85–93. doi:10.1038/nature18849

Brugiroux S, Beutler M, Pfann C, Garzetti D, Ruscheweyh HJ, Ring D, Diehl M, Herp S, Lotscher Y, Hussain S, Bunk B, Pukall R, Huson DH, Munch PC, McHardy AC, McCoy KD, Macpherson AJ, Loy A, Clavel T, Berry D, Stecher B. 2016. Genome-guided design of a defined mouse microbiota that confers colonization resistance against Salmonella enterica serovar Typhimurium. *Nat Microbiol* **2**:16215. doi:10.1038/nmicrobiol.2016.215

Chatzidaki-Livanis M, Geva-Zatorsky N, Comstock LE, Hooper L V. 2016. Bacteroides fragilis type VI secretion systems use novel effector and immunity proteins to antagonize human gut Bacteroidales species. *Proc Natl Acad Sci U S A* **113**:3627–3632. doi:10.1073/pnas.1522510113

Cheng Q, Paszkiet BJ, Shoemaker NB, Gardner JF, Salyers AA. 2000. Integration and excision of a Bacteroides conjugative transposon, CTnDOT. *J Bacteriol* **182**:4035–43. doi:10.1128/JB.182.14.4035-4043.2000

Coward C, Restif O, Dybowski R, Grant AJ, Maskell DJ, Mastroeni P. 2014. The Effects of Vaccination and Immunity on Bacterial Infection Dynamics In Vivo. *PLoS Pathog*

10:e1004359. doi:10.1371/journal.ppat.1004359

Coyne MJ, Chatzidaki-Livanis M, Paoletti LC, Comstock LE. 2008. Role of glycan synthesis in colonization of the mammalian gut by the bacterial symbiont Bacteroides fragilis. *Proc Natl Acad Sci U S A* **105**:13099–13104. doi:10.1073/pnas.0804220105

Cremer J, Arnoldini M, Hwa T. 2017. Effect of water flow and chemical environment on microbiota growth and composition in the human colon. *Proc Natl Acad Sci U S A* **114**:6438–6443. doi:10.1073/pnas.1619598114

Cubillos-Ruiz A, Guo T, Sokolovska A, Miller PF, Collins JJ, Lu TK, Lora JM. 2021. Engineering living therapeutics with synthetic biology. *Nat Rev Drug Discov*. doi:10.1038/s41573-021-00285-3

Cullen TW, Schofield WB, Barry NA, Putnam EE, Rundell EA, Trent MS, Degnan PH, Booth CJ, Yu H, Goodman AL. 2015. Antimicrobial peptide resistance mediates resilience of prominent gut commensals during inflammation. *Science* **347**:170–175. doi:10.1126/science.1260580

Dapa T, Ramiro RS, Pedro MF, Gordo I, Xavier KB. 2022. Diet leaves a genetic signature in a keystone member of the gut microbiota. *Cell Host Microbe* **30**:183-199.e10. doi:10.1016/j.chom.2022.01.002

David LA, Maurice CF, Carmody RN, Gootenberg DB, Button JE, Wolfe BE, Ling A V., Devlin AS, Varma Y, Fischbach MA, Biddinger SB, Dutton RJ, Turnbaugh PJ. 2014. Diet rapidly and reproducibly alters the human gut microbiome. *Nature* **505**:559–563. doi:10.1038/nature12820

De Sordi L, Lourenço M, Debarbieux L. 2019. The Battle Within: Interactions of Bacteriophages and Bacteria in the Gastrointestinal Tract. *Cell Host Microbe* **25**:210–218. doi:10.1016/j.chom.2019.01.018

Di Martino ML, Ek V, Hardt WD, Eriksson J, Sellin ME. 2019. Barcoded consortium infections resolve cell type-dependent salmonella enterica serovar typhimurium entry mechanisms. *MBio* **10**. doi:10.1128/mBio.00603-19

Donaldson GP, Ladinsky MS, Yu KB, Sanders JG, Yoo BB, Chou W-C, Conner ME, Earl AM, Knight R, Bjorkman PJ, Mazmanian SK. 2018. Gut microbiota utilize immunoglobulin A for mucosal colonization. *Science* **360**:795–800. doi:10.1126/science.aaq0926

Donia MS. 2015. A Toolbox for Microbiome Engineering. *Cell Syst*. doi:10.1016/j.cels.2015.07.003

Dybowski R, Restif O, Goupy A, Maskell DJ, Mastroeni P, Grant AJ. 2015. Single passage in

mouse organs enhances the survival and spread of Salmonella enterica. *J R Soc Interface* **12**:20150702. doi:10.1098/rsif.2015.0702

Fanning S, Hall LJ, Cronin M, Zomer A, MacSharry J, Goulding D, Motherway MOC, Shanahan F, Nally K, Dougan G, Van Sinderen D. 2012. Bifidobacterial surface-exopolysaccharide facilitates commensal-host interaction through immune modulation and pathogen protection. *Proc Natl Acad Sci U S A* **109**:2108–2113. doi:10.1073/pnas.1115621109

García-Bayona L, Comstock LE. 2018. Bacterial antagonism in host-associated microbial communities. *Science* **361**. doi:10.1126/SCIENCE.AAT2456

Goodman AL, McNulty NP, Zhao Y, Leip D, Mitra RD, Lozupone CA, Knight R, Gordon JI. 2009. Identifying Genetic Determinants Needed to Establish a Human Gut Symbiont in Its Habitat. *Cell Host Microbe* **6**:279–289. doi:10.1016/j.chom.2009.08.003

Grant AJ, Restif O, McKinley TJ, Sheppard M, Maskell DJ, Mastroeni P. 2008. Modelling within-Host Spatiotemporal Dynamics of Invasive Bacterial Disease. *PLoS Biol* **6**:e74. doi:10.1371/journal.pbio.0060074

Hapfelmeier S, Stecher B, Barthel M, Kremer M, Müller AJ, Heikenwalder M, Stallmach T, Hensel M, Pfeffer K, Akira S, Hardt W-D. 2005. The Salmonella pathogenicity island (SPI)-2 and SPI-1 type III secretion systems allow Salmonella serovar typhimurium to trigger colitis via MyD88-dependent and MyD88-independent mechanisms. *J Immunol* **174**:1675–85. doi:10.4049/jimmunol.174.3.1675

Hausmann A, Böck D, Geiser P, Berthold DL, Fattinger SA, Furter M, Bouman JA, Barthel-Scherrer M, Lang CM, Bakkeren E, Kolinko I, Diard M, Bumann D, Slack E, Regoes RR, Pilhofer M, Sellin ME, Hardt WD. 2020. Intestinal epithelial NAIP/NLRC4 restricts systemic dissemination of the adapted pathogen Salmonella Typhimurium due to site-specific bacterial PAMP expression. *Mucosal Immunol* 1–15. doi:10.1038/s41385-019-0247-0

Hsieh S, Porter NT, Donermeyer DL, Horvath S, Strout G, Saunders BT, Zhang N, Zinselmeyer B, Martens EC, Stappenbeck TS, Allen PM. 2020. Polysaccharide Capsules Equip the Human Symbiont Bacteroides thetaiotaomicron to Modulate Immune Responses to a Dominant Antigen in the Intestine. *J Immunol* ji1901206. doi:10.4049/jimmunol.1901206

Kaiser P, Regoes RR, Dolowschiak T, Wotzka SY, Lengefeld J, Slack E, Grant AJ, Ackermann M, Hardt W-D. 2014. Cecum Lymph Node Dendritic Cells Harbor Slow-Growing Bacteria Phenotypically Tolerant to Antibiotic Treatment. *PLoS Biol*

12:e1001793. doi:10.1371/journal.pbio.1001793

Kaiser P, Slack E, Grant AJ, Hardt W-D, Regoes RR. 2013. Lymph Node Colonization Dynamics after Oral Salmonella Typhimurium Infection in Mice. *PLoS Pathog* **9**:e1003532. doi:10.1371/journal.ppat.1003532

Kreuzer M, Hardt W-D. 2020. How Food Affects Colonization Resistance Against Enteropathogenic Bacteria. *Annu Rev Microbiol* **74**:787–813. doi:10.1146/annurev-micro-020420-013457

Kurkjian HM, Javad Akbari M, Momeni B. 2021. The impact of interactions on invasion and colonization resistance in microbial communities. *PLoS Comput Biol* **17**:e1008643. doi:10.1371/journal.pcbi.1008643

Li H, Limenitakis JP, Fuhrer T, Geuking MB, Lawson MA, Wyss M, Brugiroux S, Keller I, Macpherson JA, Rupp S, Stolp B, Stein J V., Stecher B, Sauer U, McCoy KD, Macpherson AJ. 2015. The outer mucus layer hosts a distinct intestinal microbial niche. *Nat Commun* **6**:1–13. doi:10.1038/ncomms9292

Li Y, Thompson CM, Trzciński K, Lipsitcha M. 2013. Within-host selection is limited by an effective population of Streptococcus pneumoniae during nasopharyngeal colonization. *Infect Immun* **81**:4534–4543. doi:10.1128/IAI.00527-13

Lim B, Zimmermann M, Barry NA, Goodman AL. 2017. Engineered Regulatory Systems Modulate Gene Expression of Human Commensals in the Gut. *Cell* **169**:547-558.e15. doi:10.1016/j.cell.2017.03.045

Lim CH, Voedisch S, Wahl B, Rouf SF, Geffers R, Rhen M, Pabst O. 2014. Independent Bottlenecks Characterize Colonization of Systemic Compartments and Gut Lymphoid Tissue by Salmonella. *PLoS Pathog* **10**:e1004270. doi:10.1371/journal.ppat.1004270

Maier L, Diard M, Sellin ME, Chouffane E-S, Trautwein-Weidner K, Periaswamy B, Slack E, Dolowschiak T, Stecher B, Loverdo C, Regoes RR, Hardt W-D. 2014. Granulocytes impose a tight bottleneck upon the gut luminal pathogen population during Salmonella typhimurium colitis. *PLoS Pathog* **10**:e1004557. doi:10.1371/journal.ppat.1004557

Maier L, Vyas R, Cordova CD, Lindsay H, Schmidt TSB, Brugiroux S, Periaswamy B, Bauer R, Sturm A, Schreiber F, Von Mering C, Robinson MD, Stecher B, Hardt WD. 2013. Microbiota-derived hydrogen fuels salmonella typhimurium invasion of the gut ecosystem. *Cell Host Microbe* **14**:641–651. doi:10.1016/j.chom.2013.11.002

Martens EC, Roth R, Heuser JE, Gordon JI. 2009. Coordinate regulation of glycan degradation and polysaccharide capsule biosynthesis by a prominent human gut

symbiont. *J Biol Chem* **284**:18445–18457. doi:10.1074/jbc.M109.008094

Mimee M, Tucker AC, Voigt CA, Lu TK. 2015. Programming a Human Commensal Bacterium, Bacteroides thetaiotaomicron, to Sense and Respond to Stimuli in the Murine Gut Microbiota. *Cell Syst* **1**:62–71. doi:10.1016/J.CELS.2015.06.001

Moor K, Diard M, Sellin ME, Felmy B, Wotzka SY, Toska A, Bakkeren E, Arnoldini M, Bansept F, Co AD, Voller T, Minola A, Fernandez-Rodriguez B, Agatic G, Barbieri S, Piccoli L, Casiraghi C, Corti D, Lanzavecchia A, Regoes RR, Loverdo C, Stocker R, Brumley DR, Hardt WD, Slack E. 2017. High-avidity IgA protects the intestine by enchaining growing bacteria. *Nature*. doi:10.1038/nature22058

Nguyen BD, Cuenca V M, Hartl J, Gül E, Bauer R, Meile S, Rüthi J, Margot C, Heeb L, Besser F, Escriva PP, Fetz C, Furter M, Laganenka L, Keller P, Fuchs L, Christen M, Porwollik S, McClelland M, Vorholt JA, Sauer U, Sunagawa S, Christen B, Hardt W-D. 2020. Import of Aspartate and Malate by DcuABC Drives H2/Fumarate Respiration to Promote Initial Salmonella Gut-Lumen Colonization in Mice. *Cell Host Microbe* **27**:922-936.e6. doi:10.1016/j.chom.2020.04.013

Nikolich MP, Shoemaker NB, Salyers AA. 1992. A Bacteroides tetracycline resistance gene represents a new class of ribosome protection tetracycline resistance. *Antimicrob Agents Chemother* **36**:1005–12. doi:10.1128/AAC.36.5.1005

Pham HL, Ho CL, Wong A, Lee YS, Chang MW. 2017. Applying the design-build-test paradigm in microbiome engineering. *Curr Opin Biotechnol*. doi:10.1016/j.copbio.2017.03.021

Pielou EC. 1966. The measurement of diversity in different types of biological collections. *J Theor Biol* **13**:131–144. doi:10.1016/0022-5193(67)90048-3

Porter NT, Canales P, Peterson DA, Martens EC. 2017. A Subset of Polysaccharide Capsules in the Human Symbiont Bacteroides thetaiotaomicron Promote Increased Competitive Fitness in the Mouse Gut. *Cell Host Microbe* **22**:494-506.e8. doi:10.1016/j.chom.2017.08.020

Porter NT, Hryckowian AJ, Merrill BD, Fuentes JJ, Gardner JO, Glowacki RWP, Singh S, Crawford RD, Snitkin ES, Sonnenburg JL, Martens EC. 2020. Phase-variable capsular polysaccharides and lipoproteins modify bacteriophage susceptibility in Bacteroides thetaiotaomicron. *Nat Microbiol* 1–12. doi:10.1038/s41564-020-0746-5

Porter NT, Luis AS, Martens EC. 2018. Bacteroides thetaiotaomicron. *Trends Microbiol* **26**:966–967. doi:10.1016/J.TIM.2018.08.005

Porter NT, Martens EC. 2017. The Critical Roles of Polysaccharides in Gut Microbial Ecology and Physiology. *Annu Rev Microbiol* **71**:349–369. doi:10.1146/annurev-micro-102215-095316

Rogers TE, Pudlo NA, Koropatkin NM, Bell JSK, Moya Balasch M, Jasker K, Martens EC. 2013. Dynamic responses of Bacteroides thetaiotaomicron during growth on glycan mixtures. *Mol Microbiol* **88**:876–890. doi:10.1111/mmi.12228

Sheth RU, Cabral V, Chen SP, Wang HH. 2016. Manipulating Bacterial Communities by in situ Microbiome Engineering. *Trends Genet*. doi:10.1016/j.tig.2016.01.005

Stecher B. 2021. Establishing causality in Salmonella-microbiota-host interaction: The use of gnotobiotic mouse models and synthetic microbial communities. *Int J Med Microbiol* **311**:151484. doi:10.1016/j.ijmm.2021.151484

Stecher B, Chaffron S, Käppeli R, Hapfelmeier S, Freedrich S, Weber TC, Kirundi J, Suar M, McCoy KD, von Mering C, Macpherson AJ, Hardt W-D. 2010. Like will to like: abundances of closely related species can predict susceptibility to intestinal colonization by pathogenic and commensal bacteria. *PLoS Pathog* **6**:e1000711. doi:10.1371/journal.ppat.1000711

Stecher B, Macpherson AJ, Hapfelmeier S, Kremer M, Stallmach T, Hardt W-D. 2005. Comparison of Salmonella enterica serovar Typhimurium colitis in germfree mice and mice pretreated with streptomycin. *Infect Immun* **73**:3228–41. doi:10.1128/IAI.73.6.3228-3241.2005

Vlazaki M, Huber J, Restif O. 2019. Integrating mathematical models with experimental data to investigate the within-host dynamics of bacterial infections. *Pathog Dis* **77**. doi:10.1093/femspd/ftaa001

Vlazaki M, Rossi O, Price DJ, McLean C, Grant AJ, Mastroeni P, Restif O. 2020. A data-based mathematical modelling study to quantify the effects of ciprofloxacin and ampicillin on the within-host dynamics of Salmonella enterica during treatment and relapse. *J R Soc Interface* **17**:20200299. doi:10.1098/rsif.2020.0299

Wang J, Shoemaker NB, Wang GR, Salyers AA. 2000. Characterization of a Bacteroides mobilizable transposon, NBU2, which carries a functional lincomycin resistance gene. *J Bacteriol* **182**:3559–71.

Wexler AG, Bao Y, Whitney JC, Bobay LM, Xavier JB, Schofield WB, Barry NA, Russell AB, Tran BQ, Goo YA, Goodlett DR, Ochman H, Mougous JD, Goodman AL, Isberg RR. 2016. Human symbionts inject and neutralize antibacterial toxins to persist in the gut. *Proc Natl Acad Sci U S A* **113**:3639–3644. doi:10.1073/pnas.1525637113

Whitaker WR, Shepherd ES, Sonnenburg JL. 2017. Tunable Expression Tools Enable Single-Cell Strain Distinction in the Gut Microbiome. *Cell* **169**:538-546 e12. doi:10.1016/j.cell.2017.03.041

Wotzka SY, Kreuzer M, Maier L, Arnoldini M, Nguyen BD, Brachmann AO, Berthold DL, Zünd M, Hausmann A, Bakkeren E, Hoces D, Gül E, Beutler M, Dolowschiak T, Zimmermann M, Fuhrer T, Moor K, Sauer U, Typas A, Piel J, Diard M, Macpherson AJ, Stecher B, Sunagawa S, Slack E, Hardt W-D. 2019. Escherichia coli limits Salmonella Typhimurium infections after diet shifts and fat-mediated microbiota perturbation in mice. *Nat Microbiol*. doi:10.1038/s41564-019-0568-5

Wotzka SY, Nguyen BD, Hardt WD. 2017. Salmonella Typhimurium Diarrhea Reveals Basic Principles of Enteropathogen Infection and Disease-Promoted DNA Exchange. *Cell Host Microbe* **21**:443–454. doi:10.1016/j.chom.2017.03.009

Supplementary Information

Supplementary Table 1: Bacterial strains

Strain	Genotype	Description	Reference
B.theta WT	ATCC 29148 *tdk-*	Parent strain of *B. theta*. Used to generate wild-type CPS mutants in this study.	(Porter et al., 2017)
B. theta acapsular	*tdk- Δcps1-8*	Acapsular *B. theta* with deletion of capsular polysaccharide locus. Used to generate acapsular mutants in this study.	(Porter et al., 2017)
B. theta-EryR WT tagged1/2/11	*tdk- :: pNBU2-cat-ermG-GFP-WITS1/2/11*	*B.theta* WT strain isogenic tag insert; fluorescent tag; erythromycin resistant	This study
B. theta-EryR WT tagged17/19/21	*tdk- :: pNBU2-cat-ermG-mCherry-WITS17/19/21*	Wild type CPS strain with isogenic tag insert; fluorescent tag; erythromycin resistant	This study
B. theta-EryR acapsular tagged 1/2/11	*tdk- Δcps1-8 :: pNBU2-cat-ermG-GFP-WITS1/2/11*	Acapsular strain with isogenic tag insert; fluorescent tag; erythromycin resistant	This study
B. theta-EryR acapsular tagged17/19/21	*tdk- Δcps1-8 :: pNBU2-cat-ermG-mCherry-WITS17/19/21*	Acapsular strain with isogenic tag insert; fluorescent tag; erythromycin resistant	This study
B.theta-TetR WT	*tdk- :: pNBU2-bla-tetQb*	Untagged strain. Wild type strain with fluorescent insert; tetracycline resistant	This study
B.theta-TetR acapsular	*tdk- Δcps1-8 :: pNBU2-bla-tetQb*	Untagged strain. Acapsular strain with fluorescent insert; tetracycline resistant	This study
Stm SL1344$^{\Delta SPI-2}$ (M3103)	*ΔssaV*	Attenuated *Salmonella enterica* serovar Typhimurium; SPI-2 KO	

Supplementary Table 2: Primers

Primer	Sequence	Use
WITS01	acgacaccactccacaccta	Forward primer. Quantification of tagged strain
WITS02	acccgcaataccaacaactc	Forward primer. Quantification of tagged strain
WITS11	atcccacacactcgatctca	Forward primer. Quantification of tagged strain
WITS17	tcaccagcccacccctca	Forward primer. Quantification of tagged strain
WITS19	gcactatccagccccataac	Forward primer. Quantification of tagged strain
WITS21	acaaccaccgatcactctcc	Forward primer. Quantification of tagged strain
ydgA	ggctgtccgcaatgggtc	Common reverse primer. Quantification of tagged strain

Supplementary Table 3: Microbiota composition in gnotobiotic mice LCM, OligoMM-12

Low complexity microbiota

OTU	Relative abundance	8 ASF species match	SILVA best match
1	6,43E-01	Bacteroides sp. ASF519	Parabacteroides goldsteinii dnLKV18
2	1,65E-01	Clostridium sp. ASF502	Clostridiales bacterium
3	9,60E-02	Eubacterium plexicaudatum strain ASF 492	Lachnospiraceae bacterium 6_1_63FAA
4	5,56E-02	Eubacterium plexicaudatum strain ASF 492	Blautia
5	2,00E-02	*	Turicibacter sp. LA61
6	8,52E-03	Eubacterium plexicaudatum strain ASF 492	Lachnoclostridium;bacterium NLAE-zl-411
7	7,40E-03	Bacterium ASF500	Flavonifractor;human gut metagenome

OligoMM12

OTU	Strain ID	DSM number	Phyla	Classification
1	YL2	26074	Actinobacteria	*Bifidobacterium longum subsp. animalis*
2	YL27	28989	Bacteroidetes	'Muribaculum intestinale'
3	I48	26085	Bacterioidetes	'Bacteroides caecimuris'
4	YL45	26109	Proteobacteria	'Turicimonas muris'
5	YL44	26127	Verrucomicrobia	*Akkermansia muciniphila*
6	KB1	32036	Firmicutes	*Enterococcus faecalis*
7	I49	32035	Firmicutes	*Lactobacillus reuteri*
8	YL32	26114	Firmicutes	*Clostridium clostridioforme*
9	YL58	26115	Firmicutes	*Blautia coccoides*
10	YL31	26117	Firmicutes	*Flavonifractor plautii*
11	KB18	26090	Firmicutes	'Acutalibacter muris'
12	I46	26113	Firmicutes	*Clostridium innocuum*